Archives of Computational Methods in Engineering manuscript No.
(will be inserted by the editor)

A review on thermo-mechanical modelling of arch dams during construction and operation. Effect of the reference temperature on the stress field

Fernando Salazar · David J. Vicente · Joaquín Irazábal · Ignasi de-Pouplana · Javier San Mauro

Received: date / Accepted: date

Abstract Double-curvature dams are unique structures for several reasons. Their behaviour changes significantly after joint grouting, when they turn from a set of independent cantilevers into a monolithic structure with arch effect. The construction process has a relevant influence on the stress state, due to the way in which self-weight loads are transmitted, and to the effect on the dissipation of the hydration heat. Temperature variations in the dam body with respect to those existing at joint grouting generate thermal stresses that may be important in the stress state of the structure. It is thus essential to have a realistic estimate of this thermal field, also called reference or closing temperature. In this work, the factors involved in the calculation of the reference temperature of double-curvature arch dams are analysed: material properties, boundary conditions and numerical aspects. First, a critical review of the state of the art is made with respect to the criteria used by various authors for decision-making in the construction of the model. Next, specific analyses are made on the effect of some important elements: the time step, the size of the domain of analysis and the methodology used for the calculation of the reference temperature. The results show the relevance of a correct calculation of the closing temperature to adequately determine the stress state of the structure.

Keywords First keyword · Second keyword · More

F. Salazar
CIMNE – Centre Internacional de Metodes Numerics en Enginyeria
Tel.: +34-93-401-74-95
E-mail: fsalazar@cimne.upc.edu

D. J. Vicente
CIMNE – Centre Internacional de Metodes Numerics en Enginyeria
Tel.: +34-93-401-74-95
E-mail: djvicente@cimne.upc.edu

J. Irazábal
CIMNE – Centre Internacional de Metodes Numerics en Enginyeria
Tel.: +34-93-401-74-95
E-mail: jirazabal@cimne.upc.edu

I. de-Pouplana
CIMNE – Centre Internacional de Metodes Numerics en Enginyeria
Tel.: +34-93-401-74-95
E-mail: ipouplana@cimne.upc.edu

J. San Mauro
CIMNE – Centre Internacional de Metodes Numerics en Enginyeria
Tel.: +34-93-401-74-95
E-mail: jsanmauro@cimne.upc.edu

1 Introduction

Thermal effects are highly relevant in the performance of concrete dams, both during construction and operation. At early stages, concrete cracking can occur due to the hydration heat generated by the exothermic reactions that take place during concrete curing. In structural elements with large thickness, where certain areas are far from the environment, the dissipation of such heat is difficult, therefore the risk of cracking increases. This effect is well known in concrete dam engineering, where the placing temperature of the concrete is frequently controlled with cooling pipes or similar devices [66].

Gravity and arch dams are typically built in separated vertical blocks of around 15 m width. Its construction is planned with different raising velocities to favour heat dissipation as the area in contact with the surrounding air is increased. By contrast, in

roller-compacted-concrete (RCC) dams, the construction process requires that the whole dam body is built at the same pace (typically high, since that is the main advantage of this technology, resulting in reduced construction time), thus reducing the heat dissipation and increasing the cracking potential. This requires specific measures to control the temperature gradients [76].

The thermal loading is also relevant during normal operation in double-curvature arch dams [88]. During this period, seasonal temperature variations can occur resulting in significant displacements and even dam cracking [73]. The structure becomes monolithic after joint grouting, thus hyperstatic [106] [48]. This implies that its response to both mechanical and thermal loading is affected. Indeed, changes in temperature with respect to that at the time of grouting generate thermal stresses and have an influence in the overall response, since joints may open in case of temperature decrease [13].

A proper definition of the reference temperature, i.e. concrete temperature at joint grouting, is essential to obtain an accurate stress field of the structure in thermo-mechanical numerical analysis [105]. Usually, a unique value for the whole dam body is applied [6, 95]. However, that may result in substantial differences between the estimated stress field and the actual state of the structure, both in ordinary and accidental scenarios.

The raising number of published works related to the thermal loading effect shows its importance in the dam engineering community. However, these works are limited either to the construction [18, 97] or to the operation period [34, 40, 87]. While the first focus on the detailed consideration of the evolution of concrete properties at early stages [11, 18, 27], those dealing with the performance during normal operation emphasise the assessment of specific thermal processes such as heat exchange by night cooling [89], the effect of solar radiation or shadows [52, 77, 78].

The thermo-mechanical analysis of arch dams during construction and operation involves a number of challenging issues to be addressed by the modeller. The design of a robust numerical model essentially depends on the available information (material properties, construction process) and on the scope of its application (construction, operation). However, computational cost is always relevant [48]. In this article, we present a critical review of the criteria followed by different authors in the solution of each of the issues involved in thermo-mechanical analysis of arch dams. Also, other parameters are further analysed to showcase their effect in the results: the time step, the computational analysis and the time integration.

In addition, we present a computational framework based on an in-house implementation of the finite element method (FEM) specifically designed to model the whole life cycle of double-curvature arch dams, considering both the construction and operation periods. Finally, a case study is presented and used to showcase the effect that a detailed determination of the reference temperature has on the stress field during operation.

The paper is organised as follows: Section 2 includes the literature review, with emphasis on key computational aspects. In Section 3, we describe our methodology and FEM implementation, as well as the case study. Results are presented and discussed in Section 4. Finally, some conclusions and recommendations are included in Section 5.

2 Review of the computational aspects of the thermo-mechanical modelling of arch dams

Table 1 contains a selection of relevant works published over the last ten years, including some real cases. In addition to the authors and the references, it includes the name, location and type of the dam analysed, as well as the phase of the dam's life cycle that is considered: construction, first filling of the reservoir and operation.

This table shows that the number of studies published on this subject increased in recent years. This may be due to the increasing capabilities of the numerical models to simulate this type of phenomena, including complex and detailed thermal processes.

Another interesting aspect shown in Table 1 is that arch dams are the most frequently analysed typology. This can be attributed to the great importance of thermal loads on the structural behaviour of this type of infrastructure, but also to the proliferation of arch dams in China [66, 69, 70], where a significant number of them have been built in recent years, most of which feature great height.

In relation to the phases of the dam's life cycle, construction, first filling and operation are considered in a similar number of works. As will be discussed throughout this study, the predominant thermal processes in each of these phases are quite different and must be taken into account when building the numerical model.

Table 1 Review summary. Case studies.

Id	First author	Year	Dam(s)	Country	Typology	Construction	First filling	Operation
0	(*This study*)	2020	Baserca	Spain	Arch	X	X	X
1	Malm [74]	2020	*Not specified*	Sweden	Arch	-	-	X
2	Ponce-Farfán [83]	2020	Enciso	Spain	RCC	X	-	-
3	Shen [93]	2020	*Not specified*	China	Gravity	-	-	X
4	Bayagoob [14]	2019	Al-Khanaq	Saudi Arabia	RCC	X	X	X
5	Belmokre [15]	2019	Tichy Haf	Algeria	Arch	-	-	X
6	Conceicão [27, 28]	2019,2017	*Not specified*	Portugal	Arch	X	-	-
7	Khaneghahi [54]	2019	Dez	Iran	Arch	X	X	-
8	Leitão [63]	2019	Foz Tua	Portugal	Arch	-	X	-
9	Soltani [95]	2019	Karaj	Iran	Arch	-	-	X
10	Alembagheri [6]	2018	Morrow Point	USA	Arch	X	X	X
11	Castilho [18, 19]	2018,2015	Alqueva	Portugal	Arch	X	-	-
12	Sayed-Ahmed [90]	2018	Muzdalifah	Saudi Arabia	Gravity	X	-	-
13	Stolz [96]	2018	Schluchsee	Germany	Gravity	-	-	X
14	Tatin [99]	2018	*Not specified*	France	Arch	-	-	X
15	Wang [108, 109]	2018,2015	Jiexu	China	Gravity	X	X	-
16	Enzel, Hjalmarsson [34, 40]	2017,2017	*Not specified*	Sweden	Arch	-	-	X
17	Li [66]; [65]	2016,2014	Xiluodu	China	Arch	X	X	-
18	Andersson [8]	2015	*not specified*	Sweden	Arch	-	-	X
19	Leitão [61]	2015	Alto Ceiro II	Portugal	Arch	-	X	-
20	Liu [69]	2015	Dagangshan	China	Arch	X	-	-
21	Liu [70]	2015	Jinpin-1	China	Arch	-	X	-
22	Liu [70]	2015	Laxiwa	China	Arch	-	X	-
23	Tatin [98]	2015	Izourt	France	Gravity	-	-	X
24	Abdulrazeg [1]	2014	Karun III	Iran	RCC-Arch	X	-	-
25	Mirzabozorg [77]	2014	Dez	Iran	Arch	-	-	X
26	Santillán [89]	2014	La Baells	Spain	Arch	-	-	X
27	Hariri [39]	2013	Dez	Iran	Arch	-	-	X
28	Yang [111]	2012	*Not specified*	China	Arch	X	-	-
29	Leitão [62]	2011	Alto Lindoso	Portugal	Arch	-	-	X
30	Jin [52]	2010	*Not specified*	China	Arch	-	-	X
31	Kuzmanovic [55]	2010	Platanovryssi	Greece	RCC	X	X	X

2.1 Governing equations

Coupled thermo-mechanical analysis of structures is complex. Problems where both mechanical and thermal processes have a similar relevance (e.g. metal forming, additive manufacturing) need to be solved with a fully-coupled approach. Nevertheless, whenever the effect of one of the components is much greater than the other, a one-way coupling strategy is perfectly valid to achieve accurate results. This is the case of concrete dams where, excluding cases facing extreme temperatures [100], deformations under ordinary loads remain small when compared to the scale of the domain. Therefore, temperature variations have a relevant influence on the mechanical response of the dam, but their deformations do not affect the thermal solution.

For the thermal part, the heat equation is solved in order to model the diffusion of the temperature field throughout the domain. Considering a continuum isotropic medium with no energy generation and constant properties, the equation for the conservation of energy reads:

$$\frac{\lambda}{\rho c}\left(\frac{\partial^2 T}{\partial x^2}+\frac{\partial^2 T}{\partial y^2}+\frac{\partial^2 T}{\partial z^2}\right)=\frac{\partial T}{\partial t} \tag{1}$$

where λ is the thermal conductivity, ρ is the density, and c is the specific heat of the material. T and t are temperature and time respectively.

Eq. (1) must be supplemented by suitable boundary conditions:

$$\begin{aligned} T - T^p &= 0 \qquad \text{on} \quad \Gamma_T \\ q_n - q_n^p &= 0 \qquad \text{on} \quad \Gamma_q \end{aligned} \tag{2}$$

with

$$q_n = q_i n_i \ , \ q_i = \lambda \frac{\partial T}{\partial x_i}$$

In eq. (2), T^p and q^p are the prescribed values of the temperature and the outgoing flux at the Dirichlet and Neumann boundaries Γ_T and Γ_q, respectively, and n_i is the unit vector normal to the boundary.

The mechanical response of the dam is governed by the following balance of momentum equation:

$$\frac{\partial \sigma_{ij}}{\partial x_j} + \rho b_i = \rho \ddot{u}_i \tag{3}$$

where σ_{ij} is the stress tensor, b_i is the body force per unit mass, and $\ddot{u}_i$ is the acceleration vector [31].

The boundary conditions for eq. (3) are specified as:

$$\begin{aligned} u_i &= u_i^p \quad \text{on} \quad \Gamma_u \\ \sigma_{ij} n_j &= s_i^p \quad \text{on} \quad \Gamma_s \end{aligned} \tag{4}$$

where u^p and s^p are the prescribed displacement and surface tractions at the Dirichlet and Neumann boundaries Γ_u and Γ_s, respectively.

2.2 Construction process: Mechanical problem

Double-curvature arch dams are built by means of separated monoliths that are later grouted to achieve three-dimensional performance through arch effect. Therefore, the response of the structure radically changes with joint grouting, which has a great influence on the stress distribution. This has implications in the determination of the stress field due to self-weight, especially when cantilevers feature high curvature in the downstream direction or in case of staged grouting [48]. In the first case, the deformations of the cantilevers due to self-weight tend to put them in contact with adjacent blocks, thus generating some arch effect even before grouting. In the latter, the gravity loads are sequentially generated on a changing structure, which evolves from a set of independent cantilevers to be partially monolithic, until last grouting completes the development of the full arch effect. These intermediate situations need to be accounted for in the determination of the stress field due to self-weight. Such effect was studied in the frame of super-high arch dams, where staged grouting is compulsory [70].

Several approaches can be found in the literature to compute self-weight (also termed dead weight or gravity load). Some authors mention the possibility of neglecting the construction process and compute the gravity load with a monolithic model [38, 70, 72, 105], but they all agree in its lack of accuracy and possibility of over or under-estimated stresses. Indeed, the consideration of the construction and grouting sequence is already recommended in historical manuals [106].

A more precise, but also simple method consists in considering independent cantilevers to compute the self-weight. This method is accurate in case blocks are not expected to be in contact during construction. Akbari *el al.* [5] used this approach in combination with staged grouting.

Interaction between cantilevers during construction can be considered with joint elements. Although tensile strength is low or even null before grouting, the use of this kind of elements yields more realistic deformations and thus in principle more accurate stress distribution. On the other hand, joint elements are non-linear [84, 110] and may lead to convergence problems and uncertainty on results accuracy, since real state of transverse joints is difficult to assess [70]. Hence, the consideration of opening and closing joints should be approached with caution and with a contrasted joint model. However, this method is recommended in some guidelines [72] and by some authors who advise the calculation of the joint elements to obtain a realistic estimate of the stresses at the end of the construction phase [13, 70].

Therefore, a suitable approach may involve calculating self-weight by considering independent cantilevers, and analysing the resulting displacements. This procedure may be valid if the shape of the dam prevents the blocks to tend to be in contact. It should be remembered that the displacements by self-weight during construction are corrected as the work progresses, and therefore the transmission of stresses between cantilevers is actually lower than the theoretical calculated without considering the construction process. This also applies to vertical displacements, which are often be neglected at the end of the construction.

2.3 Construction process: Thermal problem

The detailed consideration of the construction process is essential for a realistic estimate of the reference temperature. It implies a high computational cost [55], since a fine mesh is required to model each lift, a long transient analysis is needed, and the time step is limited to achieve convergence and obtain accurate results.

Throughout the construction process, the complete geometry of the dam body and its evolution during building need to be considered, as well as the joint grouting. Cantilevers are typically assumed to allow heat transfer, since each block is normally cast against the adjacent ones [35, 47].

The process is also affected by the boundary conditions, which vary as the building evolves [18, 22]. On those faces of each lift exposed to the environment, either permanently or temporarily, a flux exchange

with the environment should be imposed. From the point of view of the thermal phenomenon, this process is the same both in the construction and the operation stages. Therefore, comprehensive description of this processes can be found in its corresponding section (see 2.4.1). However, a particular feature of the construction phase in relation to the thermal flux between the dam and the environment is the consideration of the placement of formworks on each lift. This effect was simulated by some authors with the resulting attenuation of heat exchange [18, 27].

The thermal phenomena involved only in the constructive stage, or at least in a predominant way, are analysed in this section: concrete placement temperature, hydration heat generation and the use of measures to control concrete temperature (with special focus in the case of arch dams in pipe-cooling methods).

2.3.1 Concrete placement temperature

The thermal evolution of concrete, both in short and long terms, is influenced by the initial or placement temperature. Ideally, this temperature should be low enough so that the rise due to hydration of the cement would just bring the concrete temperature up to its final stable state, avoiding volumetric temperature shrinkage that causes cracking [105]. However, this ideal situation is unfeasible in many real cases.

The placement temperature is often controlled in-situ and even limited by the construction regulations to prevent large temperature gradients [2, 18, 22, 103]. When detailed information is available on these control measures, an accurate value can be used in the numerical model. This applies to models generated before construction, in case the requirements are known, and to those used for retrospective analysis, if such control was performed on site and the information is available [55]. In absence of such detailed information, the initial concrete temperature needs to be estimated.

In RCC dams, the temperature of the concrete mixture when poured has a great influence on the construction phase, so many research efforts focused on the precise definition of this variable in numerical calculations. Noorzaei *et al.* [80] took a value of 30 ℃ for all RCC lifts, as the specifications in that work (construction of Kinta dam in Malaysia) read that the placing temperature was maintained below 30 ℃. Luna *et al.* [71], on the other hand, set the initial temperature of each lift to be equal to the air temperature at the time of pouring. Similarly, Cervera *et al.* [25] took the placing temperature of each lift as equal to the ambient temperature increased in 5 ℃. This increment is assumed to be due to the stocking conditions and the manipulation operations performed during the production process of the concrete. Jaafar *et al.* [51] also defined the placement temperature as a function of the ambient temperature, with variable increase for each season.

The importance of the concrete placement temperature in other types of concrete dams has also been analysed. In most of these studies, it was assumed to be a function of the air temperature, but different assumptions have been made for each case. Araujo *et al.* [9] considered that the temperature of the rock and the water forming the concrete mixture were equal to the mean temperature of the location during the last ten years. On the other hand, Castilho *et al.* [18] considered a placement temperature equal to that of the air on site, limited to the temperature interval prescribed by the Portuguese regulations (7.25 ℃). Cervera and García-Soriano [22] followed a similar approach, but increased the air temperature by 2 ℃ and 4.5 ℃ in winter and summer, respectively, to implicitly consider the effect of radiation and insolation, while Yang *et al.* [111] took into account the effect of solar radiation through increasing ambient temperature by 2 ℃ all the year, based on the recommendations of the Chinese Ministry of Water Resources. Meanwhile, Honorio *et al.* [41] took the ambient temperature plus 5 ℃, assuming that this increment accounted for the initial hydration reactions and likely increasing of temperature due to the transport of concrete, as the Japan Concrete Institute suggests. By its part, Conceição *et al.* [27] used an estimate based on the temperature of the concrete mixture and the prescribed limits (5 ℃ and 25 ℃) [46].

A similar criterion was used by Briffaut *et al.* [16], based in turn on the proposal of Torrenti and Buffo-Laccarriere [102]: a linear relation between external temperature (T_{air}) and initial concrete temperature ($T_{c,0}$) was taken. They fitted the parameters of the linear function from experimental data taken in two different sites (with T_{air} and $T_{c,0}$ in ℃), leading to [16]:

$$T_{c,0} = 0.6 \cdot T_{air} + 10.9 \tag{5}$$

This assumption is based on the fact that aggregates are often stored outdoors, hence their temperature is influenced by that of the air on site. Therefore, it should be applied with caution in other settings.

2.3.2 Hydration heat generation

The behaviour of concrete at early stages has been deeply studied in different areas of civil engineering. The temperature increase due to the cement curation is well known and leads to adopting measures to alleviate the thermal gradients that may cause cracking. In dam engineering, cooling pipes and concrete precooling are often used for such purpose.

In numerical simulations, the proper characterisation of the hydration heat is essential when analysing the first stages of concrete after pouring. If the focus is placed on the operation stage, hydration heat is frequently neglected, especially in thin arch dams [95].

The rate of generation of hydration heat strongly depends on the particular properties of the mixture. Azenha [11] performed an experimental campaign of the behaviour of different cements typically used in Portugal. Castilho *et al.* [18] included a comprehensive review of the modelling approaches to this phenomenon, which range from analytical expressions developed to fit observed evolution of temperature assuming adiabatic conditions [45, 50, 51, 71, 80] to complex thermo-chemical models as that proposed by Cervera *et al.* [23, 24], based on the work by Ulm and Coussy [104].

In concrete dams, large areas are typically exposed to the environment. In those areas in contact to or near the surrounding air the process is non-adiabatic. The non-adiabatic formulation presented by Reinhardt *et al.* [85] suggests that the heat generation rate depends not only on the properties of the concrete mixture, but also on its temperature and hardening state.

In order to take into account these features, the degree of reaction (r) can be calculated as

$$r = \frac{Q(t)}{Q_{max}} \tag{6}$$

where Q_{max} is the total heat of hydration (measured at 90 days) and $Q(t)$ the amount of heat generated until time t.

The rate of heat generation as a function of r was analysed by Reinhardt *et al.* [85]. They conclude, from laboratory measurements in different cements, that their relation can be fitted by the following normalised function which depends on four constants (A, B, C and D).

$$f(r) = \frac{q}{q_{max}} = Ar^2 e^{(-Br^3)} + Cre^{(-Dr)} \tag{7}$$

In addition, the heat generation is also affected by the temperature of the concrete on the hydration process. The maximum heat generation rate at temperature T can be computed as follows

$$g(T) = Ke^{\frac{-E_a}{RT}} \tag{8}$$

being K a rate constant in $\mathrm{W/m^3}$, E_a the apparent activation energy in J/mol, and R the ideal gas constant in $\mathrm{J/(mol \cdot K)}$.

The hydration heat is then provided by:

$$Q(r, T) = f(r)g(T) \tag{9}$$

Assuming this formulation, the hydration heat Q depends on the degree of reaction and on the temperature of the concrete at time t.

In a specific analysis of concrete behaviour at early stages, Briffaut *et al.* [16] considered the thermal and mechanical response of a 2-m high, 1.2-m width wall, and concluded that the heat generation process can be considered as adiabatic at the center of such structure (e.g. 60 cm from the external surface). Ponce *et al.* [83] studied the thermal behaviour of an RCC dam using both an adiabatic and a non-adiabatic formulations. They observed that the difference between both approaches was limited to the first hours after pouring each lift, before placing the next one. In other words, the process can be considered adiabatic for all lifts except the most external one, which in this case has a relatively large surface in contact with air. In their case, the lifts were 30 cm height.

Arch dams are typically built with thicker lifts (2 m in our case study). According to the previous results, the effect of the non-adiabatic nature of the phenomenon is limited to the topmost 30-60 cm. Therefore, it could be neglected unless special interest is put on the detailed analysis of the such area.

If adiabatic conditions are assumed, the reaction only depends on time. The reaction rate is controlled by the constant parameter α, so the hydration heat can be estimated by the following exponential expression [50, 80]:

$$Q(t) = c\rho T_{max}\alpha(1 - e^{-\alpha t}) \tag{10}$$

where $Q(t)$ is the hydration heat generated at time t, c is the specific heat, ρ is the density, T_{max} is the maximum temperature reached in adiabatic conditions, which can be obtained from experimental tests (e.g. Li *et al.*, 25-27 ℃, [65]; Noorzaei [80], 18 ℃; Wang *et al.*, 23.8-26.3 [109]; Conceição, 23 ℃ [27]) and α is a parameter for the heat generation rate.

2.3.3 Measures to control concrete temperature

The importance of the concrete placement temperature in the thermal behaviour of arch dams

has already been mentioned. During construction, temperature control measures are normally used to maintain the temperature of the concrete within certain limits and avoid cracking. For this purpose, cooling pipes are frequently used to partially counteract the thermal increase due to the generation of hydration heat [12]. Cold water is circulated through these pipes that exchange heat with the concrete, reducing the maximum temperature reached.

In some cases, cooling pipes are used in two different periods, i.e., right after pouring, with the above mentioned goal, then before joint grouting. This second phase is often termed post-cooling [6, 18] and is performed to open the joints between blocks before sealing, to avoid subsequent joint opening due to temperature decrease during dam operation.

The effect of the cooling pipes needs to be considered in the numerical model to assess the thermal behaviour of concrete at early ages. Various methods have been proposed for that, with different levels of detail. Alembagheri *et al.* [6] simply assumed that the concrete temperature at joint grouting was equal to the target post-cooling temperature (17 ℃). Wang *et al.* [108] considered the effect of the cooling water as a negative heat source whose magnitude depends on the initial water temperature. Conceição *et al.* tried different strategies. Firstly, they used a very detailed numerical approach to model heat exchange between water flowing through cooling pipes and the surrounding concrete to model the initial cooling [27]. However, post-cooling was not considered due to lack of information available on the actual process followed. The deviations reported between computed and observed temperature were nonetheless attributed to the uncertainty in the date of removal of the formwork. In a subsequent work [28], they proposed a new methodology to simulate the post-cooling effect, where the heat dessipation by the cooling pipes is reproduced using fictitious convective boundaries, aiming to decrease the computational effort.

Castilho *et al.* [18] did not consider neither initial nor final cooling for the Alqueva Dam case study. They concluded that the effect of the cooling pipes at very early stages was negligible for such case, but that the lack of consideration of post-cooling was responsible for the inaccuracies observed in some areas.

Research on this field is intensive especially in China, regarding the design and construction of super-high arch dams [67]. This led to the development of very detailed approaches to account for cooling pipes in numerical models [26, 64, 111], as well as to their application to optimise the system in terms of the materials used, the water temperature, the geometry and location of the pipes, among other aspects [44, 69].

In cold climates, it may be necessary to protect freshly placed concrete to control its temperature, as in fact was done in the case study used in this work [7]. In any case, the formwork itself has an insulating effect that also affects the evolution of the temperature range. This effect is conventionally considered by modifying the convection coefficient during the period of permanence of the formwork [18, 27].

2.3.4 Summary of published works

Table 2 collects a list of case studies of real dams in which some of these processes have been treated, classified according to the approach followed to consider each process in the numerical model.

2.4 Environmental conditions

2.4.1 Dam-Air exchange fluxes

According to Agulló *et al.* [4] the thermal performance of concrete dams is influenced by the environmental conditions, the geometry and location of the dam and the thermal properties of concrete. The geometry and location of the dam can be considered as environmental conditions being mainly related to the weather, insolation and shadows.

In recent works, comprehensive methodologies have been proposed and followed considering all phenomena involved with regard to ambient flux exchanges: forced convection, long and short wave radiation, reflection coefficient of the environment, evaporation or night cooling [11, 18, 70, 77, 89]. These approaches share the need for a very detailed information on the actual environmental conditions of the site, including meteorological effects during the construction period. Nervertheless, there is a lack of standardisation in this area, which means that each study integrates different flow exchange phenomena, discarding those for which data are not available or whose information is considered unreliable. The first section of Table 3 includes those cases in which processes of heat exchange between air and pressure have been considered in the numerical models, indicating the particular phenomena integrated in each case.

Among all environmental phenomena involved, convection is one of the most influential mechanisms in the thermal response of concrete. It controls the effect of the external temperature on the temperature evolution in the dam body and depends on the wind speed, as was observed in experimental studies [58].

Table 2 Review summary. Construction processes.

Case		(a) Concrete placement temperature				(b) Hydration heat model			(c) Other relevant factors	
Id	Typology	Uniform	One for each lift	Monitored during casting	Other formulae	Adiabatic	Non-adiabatic	Simplified	Pipe-cooling	Formworks
0	Arch	-	X	-	-	X	-	-	-	-
2	RCC	-	X	-	-	X	X	-	-	-
4	RCC	-	-	-	X	X	-	-	-	-
6	Arch	-	-	-	X	-	X	-	X	X
7	Arch	-	-	-	-	-	-	X	-	-
10	Arch	-	-	-	-	-	-	X	-	-
11	Arch	-	X	-	-	X	-	-	-	X
12	Grav.	-	X	-	-	X	-	-	X	-
15	Grav.	-	X	-	-	X	-	-	X	-
17	Arch	-	-	-	-	X	-	-	X	-
20	Arch	-	-	X	-	-	X	-	X	-
24	RCC	-	X	-	-	-	X	-	-	-
28	Arch	-	X	-	-	X	-	-	X	-
31	RCC	-	X	-	-	-	X	-	-	-

(a) Concrete placement temperature methods - *Uniform*: same placement temperature for the whole dam body; *One for each lift*: function of the air temperature at the time of pouring; *Monitored during casting*: temperature measured on-site is assigned to the numerical model; *Other formulae*: use of empirical formulation based on different parameters (ambient temperature at different periods and mixture temperature). **(b) Hydration heat model -** *Adiabatic*: temperature models based on adiabatic formulation; *Non-Adiabatic*: temperature models based on non-adiabatic formulation; *Simplified*: estimation of same maximum temperature rise value for all lifts. **(c) Other relevant aspects -** *Pipe-cooloing*: simulation of the effect of artificial concrete post-cooling through embedded pipes; *Formworks*: consideration of formworks placement and removal and the different air-concrete flux coefficient of convection.

However, this variable is usually estimated by simplifications, as it undergoes relevant variations in space and time and cannot be constantly measured at every location. The daily mean velocity is often considered, sometimes in the closest station, even some kilometres away from the construction site citecastilho2018fea.

Regarding insolation, the exact trajectory of the sun throughout the year in the location of the dam can be computed and applied [18, 56], as well as the shadows [89]. However, clouds generate local modifications that are complicated to include and can strongly modify the theoretical radiation. In a specific analysis, Azenha reported deviations of ±50% [11].

In a dam under construction, these aspects could be theoretically measured and accounted for, provided that the required resources are available for installing sensors and a data acquisition system. However, even in such ideal scenario, installing a network of thermometers in the dam body would be probably more efficient to directly record the concrete temperature and compute the whole thermal field by extrapolation.

When the analysis is made in the design stage, or in retrospective analysis, the environmental conditions need to be estimated.

2.4.2 Water temperature

Water temperature is frequently taken as the imposed boundary condition on the wetted area of the upstream face of concrete dams. It is well known to vary throughout the year and in depth, although the degree of variation greatly depends on the site and operation conditions. Different approaches exist to define water temperature. Some of the most common methods are the following: assign a uniform temperature to the complete body of the reservoir (regardless its depth), define a law with different temperatures with depth based on real measurements of thermometers, or implementing empirical equations [112]. The second section of Table 3 summarizes the approaches employed in different case studies.

When temperature is recorded at different depths during the period of analysis, a polynomial can be fitted as a function of depth and interpolated over time. Terheiden *et al.* [96] applied a bilinear law, assuming constant bottom temperature equal to 4 ℃, surface temperature equal to that of air, and the records by a thermometer located at intermediate height. Moreover, Leger *et al.* [60] proposed to classify the reservoirs in two types with different temperature profiles:

1. Type I: reservoirs with small water intakes with respect to their volumes
2. Type II: reservoirs with an important water inlet with respect to their volume and usually less deep

In type I reservoirs, the law proposed by Terheiden *et al.* can be applied, while in type II the temperature distribution will be almost uniform. Other authors suggested the use of similar approaches applying

weekly or sometimes monthly mean values for the temperature imposition [3, 8, 30, 34, 40, 61, 63, 72, 79].

In the absence of measured temperature data, either because no thermometers are available or because the analysis is carried out at the design stage, there are other alternatives. Townsend [103] recommends to search information of nearby reservoirs with similar operating conditions. If no data is available at close reservoirs, the next best estimate of the reservoir temperatures would be obtained by the principle of heat continuity. This method considers the amount and temperature of the water entering and leaving the reservoir, and the heat transfer across the reservoir surface, therefore, this implies difficult calculations and requires accurate information about the temperature and flow of the river. Finally, if none of the two previous alternatives is possible, Townsend suggests to estimate the reservoir temperature based on the monthly mean air temperatures at the site, the operation and capacity of the reservoir, and the general characteristics of the river flow.

Another possibility, if there is no reliable information about the operation of the reservoir and the river flow, is the use of the analytic formulation proposed by Bofang [112]. It is a general polynomial approach based on data recorded from a set of reservoirs in China. It may offer a good approximation to the case study, but it also has limitations if the environmental conditions are highly different from such reservoirs. In spite of the limitations of this formulation, it is a useful approach and was applied in several studies to estimate the water temperature [6, 15, 39, 42, 62, 77, 78, 87–89, 92, 95].

Ardito *et al.* [10] proposed a modification to the Bofang expression that was used by Tatin *et al.* [99], while Li *et al.* [65] computed the water temperature as a function of the reservoir level and time, considering the effect of the ground temperature, which was high (around 25 ℃) for their case study (Xiluodu Dam).

2.5 Thermal characterization of concrete

Concrete thermal properties also have a great impact on the results of numerical computations. In some real projects, data is available from tests performed on site, which can be transferred to the numerical models. However, in most cases, values are either extracted directly from the specialised literature or calculated from empirical formulas that depend on a series of parameters proposed by other authors.

Table 4 includes values extracted from the real case studies analysed for the relevant thermal parameters of concrete arch dams. They are discussed in the following subsections.

2.5.1 Thermal conductivity

This is the main parameter in the computation of the effect of a change in air temperature on the thermal field in the dam body. It essentially depends on the concrete properties, and in particular on the water to cement ratio, age, type of aggregate, temperature and saturation rate. The volumetric fraction of aggregate is often around 80 %, thus its thermal properties have strong influence on the performance of the mix [11]. The overall range of variation may be established between 1.2 and 3.5 $\mathrm{W/(m \cdot K)}$. Since conductivity increases with the water content, a higher value can be expected at early stages, decreasing later with time, although such effect was found to be minor [11]. Briffaut *et al.* [16] assessed the influence of external temperature on conductivity and specific heat of concrete and found it to be also negligible. Therefore, a constant value can be employed [99].

Santillán *et al.* chose a constant value equal to 2.43 $\mathrm{W/(m \cdot K)}$ for La Baells arch dam, based on experimental tests during construction [87]. The formulators of the Tenth Benchmark Workshop on Numerical Analysis of Dams [47] suggested using 2.5 $\mathrm{W/(m \cdot K)}$.

2.5.2 Convection coefficient

Different authors used variable values, not only due to different concrete properties such as the water to cement ratio. Site conditions are highly variable among dams and different to those at laboratory: wind speed features high spatio-temporal variability and is unfeasible to measure at full detail [11]. It is therefore assumed that the existing values in the bibliography can be considered useful guidelines for their application in numerical models that allow the calculation of maximum and minimum temperatures and stresses. They can be determined from average values of wind speed [91].

For the calculation of an RCC dam in Saudi Arabia (an extremely hot arid region), Bayagoob and Bamaga [14] followed the recommendations from Duffie [33] who calculated the surface heat transfer coefficient as $h_c = 5.7 + 3.8 \cdot V_w$, being V_w the average wind speed. On the other hand, for La Baells arch dam in Spain, Santillán *et al.* [89] followed Agulló *et al.* [3] in using the expression proposed by Kehlbeck [53] to compute the convection coefficient to apply to the outer dam faces as $h_c = 3.67 + 3.83 \cdot V_w$. For the inner surfaces, e.g. those in the galleries,

Table 3 Review summary. Other thermal processes.

	(a) Dry faces						(b) Wetted faces			(c) Initial condition		
Id	Conv.	Short wave rad.	Long wave rad.	Evap.	Shadows	Bofang	Unif.	Thermo	Other	Unif.	Trans.	Monit.
0	X	-	-	-	-	-	-	X	-	-	-	-
1	X	-	-	-	-	-	X	-	-	X	-	-
2	X	X	X	X	-	-	-	-	-	-	-	-
3	X	-	-	-	-	-	-	X	-	X	-	-
4	X	X	-	-	-	-	-	-	X	-	-	-
5	X	X	X	X	X	X	-	-	-	-	X	-
6	X	X	-	-	-	-	-	-	-	-	-	-
8	X	X	X	-	-	-	-	X	-	X	-	-
9	X	X	X	-	-	X	-	-	-	X	-	-
10	X	X	-	-	-	X	-	-	-	-	-	-
11	X	X	X	-	X	-	-	-	-	-	-	-
12	X	-	-	-	-	-	-	-	-	-	-	-
13	X	X	X	X	-	-	-	-	X	-	X	-
14	X	X	X	-	-	-	-	X	X	-	-	X
15	X	X	-	-	-	-	X	-	-	-	-	-
16	X	-	-	-	-	-	X	-	-	X	-	-
17	X	-	-	-	-	-	-	-	X	-	-	-
18	X	-	-	-	-	-	-	X	-	-	X	-
19	X	X	-	-	-	-	X	-	-	-	-	-
20	X	X	-	-	-	-	-	-	-	-	-	-
23	X	-	-	-	-	X	-	-	-	-	X	-
25	X	X	X	-	-	X	-	X	-	-	X	-
26	X	X	X	X	X	X	-	-	-	-	X	-
27	X	X	-	-	-	X	-	-	-	-	-	X
28	X	X	-	-	-	-	-	-	-	-	-	-
29	X	X	-	-	-	X	-	-	-	-	X	-
30	X	X	X	-	X	-	-	X	-	-	-	X
31	X	-	-	-	-	-	-	-	-	-	-	-

(a) Dry faces - *Convection*: heat exchange caused by temperature difference between the bulk of air and the air neighboring the surface of the structure; *Short wave radiation*: energy emitted by the sun; *Long wave radiation*: difference between the long-wave radiation that is being emitted by the concrete and the incident energy being absorbed by the dam; *Evaporation*: mechanism of heat loss from water evaporation; *Shadows*: computation of shadows areas in the dam surface considering incident angle of the sun's rays. **(b) Wet faces -** *Bofang*: Bofang: Use of Bofang's formula [112] or slight variations; *Uniform*: assignment of uniform water temperature; *Thermometers*: estimation of temperature at different levels through measured data; *Others*: other methods to compute water temperature including numerical modellling, mean values, statistics based on historical data and empirical formulae). **(c) Initial condition -** *Uniform*: uniform value as initial temperature for the whole dam body; *Transient*: distributed field temperature calculated by transient analysis; *Monitored*: use of termometers embedded inside the dam.

natural convection with a constant value of 3.5 is assumed. Sheibany [92] and Alembagheri [6] chose a constant value of $h_c = 23.2$ W/(m$^2 \cdot$ K), associated to a mean wind speed of 3 m/s.

Many authors use a combined or global convection coefficient which encompasses the effects of both the convection and radiation. For instance, Castilho and Leitão *et al.* [18, 62, 63] defined a *transmission coefficient* as the sum of the convection coefficient and the radiation coefficient. This was computed with the expression proposed by Brown and Marco [17], which involves the thermal conductivity, density and absolute viscosity of air, as well as the *size of the considered flat surface*, taken as 0.60 m following Silveira [94]. The resulting convection coefficient, for an average wind speed of 2.9 m/s, is 15.2 W/(m$^2 \cdot$ K). As for the radiation coefficient, they used a constant value of 5 W/(m$^2 \cdot$ K), resulting in 20.2 W/(m$^2 \cdot$ K) to account for both effects. Similarly, Tatin *et al.* [99] defined a *global exchange coefficient*, for which a value of 40 W/(m$^2 \cdot$ K) was obtained after a calibration process. Azenha took 22 W/(m$^2 \cdot$ K) for a convection/radiation coefficient corresponding to a wind velocity of 2 m/s. The difference between authors is noticeable.

The formulators of the Tenth Benchmark Workshop on Numerical Analysis of Dams [47] suggested a constant value of 16 W/(m$^2 \cdot$ K) [35].

2.6 Numerical considerations for the thermal problem

2.6.1 Time integration scheme

The finite element method leads to a system of nonlinear partial differential equations that describe

Table 4 Review summary. Thermal concrete properties of arch dams.

Id	Conductivity [W/(m · ℃)]	Specific heat [J/(kg · ℃)]	Thermal expansion [1/℃]	Max. adiab. temp. rise [℃]	Concrete-air convection [W/(m^2 · ℃)]	Emissivity [−]	Absorption [−]
1	2	900	10^{-5}	-	13	-	-
6	2.6	-	$1.1 \cdot 10^{-5}$	-	-	-	-
7	-	-	$6 \cdot 10^{-6}$	-		-	-
8	2.33	879	10^{-5}	-	16.67	-	-
9	2.91	967	$1.02 \cdot 10^{-5}$	-	20.9	0.775	-
10	2.62	-	10^{-5}	-	23.2	-	-
11	2.62	920	-	21	15.2	-	0.65
14	-	-	10^{-5}	-	40*	-	0.65
16	2	900	10^{-5}	-	13.3	-	-
17	2.14	860	10^{-5}	25.3	12.15	0.88	-
18	1.7	1000	-	-	-	-	-
19	2.33	879	10^{-5}	-	22.2-29.4	-	0.45-0.65
20	2.64-2.78	1030-1060	8.51-8.67 10^{-6}	23.8-24.5	-	-	-
21	2.32	883	-	-	18.8	-	-
22	2.27	933	-	-	23.26	-	-
25	1.7	920	-	-	60*	0.8	0.7
26	2.43	982	10^{-5}	-	-	0.7	0.75
27	2.62	912	$6 \cdot 10^{-6}$	-	15.47	0.88	0.65
28	2.14	860	-	26	11.63	-	-
29	2.62	920	$9.5 \cdot 10^{-6}$	-	25	-	0.65
30	1.39	902.3	$8 \cdot 10^{-6}$	-	-	-	0.65
Max	2.91	1045	$1.1 \cdot 10^{-5}$	26	25.8	0.88	0.75
Min	1.4	860	$6 \cdot 10^{-6}$	21	11.63	0.7	0.55
Mean	2.29	921.31	$9.29 \cdot 10^{-6}$	24.1	17.98	0.79	0.66
Median	2.33	912	10^{-5}	24.7	16.67	0.79	0.65

* These values are not considered to compute statistics, because they consider other processes such as short and long wave radiation.

the time-dependent thermal problem. The discretized form of eq. (1) at time t_n yields:

$$\mathbf{C}\dot{\mathbf{T}}_n + \mathbf{K}\mathbf{T}_n = \mathbf{F}_h + \mathbf{F}_a \tag{11}$$

Where $\mathbf{C}$ is the specific heat matrix; $\mathbf{K}$ is the conductivity matrix and $\mathbf{F}_h$ and $\mathbf{F}_a$ are the vectors of external heat flows due to hydration heat generation and ambient temperature exchange. $\mathbf{T}_n$ is the vector of nodal temperatures and $\dot{\mathbf{T}}_n$ the rate of change of the nodal temperature values at time t_n.

The time integration of this system of equations is typically based on the finite difference discretization of the time derivative, leading to the so-called θ-methods. With such approaches, the temperature in the time step $\mathbf{T}_{n+1}$ is calculated as a function of the weighted rate of change of the nodal temperature values at time t_n and at time t_{n+1}.

$$\mathbf{T}_{n+1} = \mathbf{T}_n + (1-\theta)\Delta t\dot{\mathbf{T}}_n + \theta\Delta t\dot{\mathbf{T}}_{n+1} \tag{12}$$

From eq. (11) at time t_{n+1} and eq. (12) the following expression is derived:

$$\left(\frac{1}{\theta\Delta t}\mathbf{C} + \mathbf{K}\right)\mathbf{T}_{n+1} = \mathbf{C}\left(\frac{1}{\theta\Delta t}\mathbf{T}_n + \frac{(1-\theta)}{\theta}\dot{\mathbf{T}}_n\right) + \mathbf{F}_h + \mathbf{F}_a \tag{13}$$

Different schemes are obtained from values of $\theta \in [0,1]$:

- $\theta = 0$: Forward Euler scheme, explicit.
- $\theta = 1/2$: Crank-Nicolson scheme, implicit.
- $\theta = 2/3$: Taylor-Galerkin scheme, implicit.
- $\theta = 1$: Backward Euler scheme, implicit.

Implicit methods are unconditionally stable while explicit ones are conditionally stable and require small time steps. On the other hand, explicit methods avoid some costly computational operations like the inversion of a matrix at every time step, something that is necessary in implicit methods.

Agulló *et al.* [3] used the Forward Euler explicit scheme ($\theta = 0$) for the calculation of the transient response of a concrete dam. In their case the use of small time steps allowed close monitoring of the thermal field in the dam body. However, implicit schemes are more frequently used in the thermal analysis of dams during construction and operation, since they require the calculation of long transient analyses (typically months or even years) and therefore long time steps are advantageous to reduce the overall computational time.

Noorzaei *et al.* [80] and Abdulrazeg *et al.* [1] applied a Taylor-Galerkin approach ($\theta = 2/3$) while Santillán *et al.* [89] used a Crank-Nicolson approach. For their part, Sheibany and Ghaemian [92], Azenha [11], Kuzmanovic

et al. [55], Yang *et al.* [111], Bofang [113], Castilho *et al.* [18, 19], Conceição *et al.* [27] and Tatin *et al.* [99] applied a Backward Euler scheme ($\theta = 1$).

As we considered isotropic conductivity of concrete, there are only two sources of nonlinearity in the construction phase (heat flow from hydration heat generation and ambient temperature exchange) and one during operation (ambient temperature exchange). These nonlinearities introduce oscillations in the problem whose effects are damped with high values of θ [57]. This damping is higher for the Backward Euler scheme, whose adoption is thus advantageous when large time steps are used.

2.6.2 Computational domain

There is not an agreement on the appropriate limits of the computational domain in thermal analysis of dams. Some authors disregard an explicit modelling of the foundation by assigning boundary conditions on the foundation-dam interface. With this approach, the boundary condition on the dam-foundation interface can be defined in two ways: adiabatic with zero thermal flux assumed across the interface [19, 27, 92] or as an imposed constant temperature [10, 77]. Ardito *et al.* [10] recommend the second option, given that the first one is equivalent to assume that the thermal flux would be almost unidirectional across the dam thickness, which is unrealistic given the large dimensions of the dam basis.

Other authors explicitly considered the rock mass in the numerical model with a volume similar to that recommended for mechanical analysis: extension of the surrounding foundation (vertically and horizontally) at least equal to a characteristic dimension of the structure (i.e., the height, the width at the base or the crest length) [48, 72]. Examples of these configurations are commonly found in studies which analyse real dams [1, 36, 68, 89, 95]. In all the above cited studies, the resulting large volumes of the foundation require variable mesh size to avoid excessive number of elements.

The contributors to the Theme A in the Tenth Benchmark Workshop on Numerical Analysis of Dams [47] used half of the dam body and didn't consider the foundation ground. Although the joints were sealed during a two-months period at the end of construction, the structure was considered monolithic for both the thermal and the mechanical problems [35]. In that case, the proposers suggested to use only one mesh element for each concrete lift (hexahedral).

When the foundation is included in the model, adiabatic boundary conditions are used for the side vertical surfaces, while the bottom surface is generally assumed to have constant temperature, not affected by the environment (e.g., [18, 43, 65]).

2.7 Reference temperature

The temperature rise generated by the hydration heat results in the appearance of *self-stresses* [113] due to the non-linear temperature distribution in the concrete mass. While the inner part of the concrete mass is only affected by the hydration heat, the external regions are also influenced by the heat exchange with the environment. The ambient temperature is generally colder than that of the concrete during this process. As a result, the outer region of the concrete tends to shrink but is restricted by the inner mass, generating tensile stresses on the outside and compression on the inside. Azenha [11] studied this type of stress in great detail and concluded that it is difficult to determine the precise moment at which concrete begins to transfer stresses due to the influence of several factors, including, among others, the *placement temperature* and the types of additives added to the concrete that can accelerate or retard the setting process.

This type of thermal stresses are highly relevant in massive concrete structures featuring elements with large thickness, such as super-high arch dams or RCC dams. Therefore, specific computational procedures are often applied for detailed analysis of the thermal evolution of the concrete mass, including the design of cooling measures as described in the previous section. In conventional double-curvature arch dams, thermal stresses before joint grouting are considered of little relevance and often neglected [86]: they feature lower thickness than other dam typologies and are built in separated blocks (cantilevers), at different pace, so that heat exchange with the environment is facilitated to dissipate the hydration heat.

During normal operation, other type of thermal stresses appear [88], i.e., *restraint stresses* [113]. They occur when the deformation of the structure due to temperature variations is restricted by the mechanical boundary conditions. Conventional arch dams are built in vertical independent blocks separated by joints contained in radial vertical planes. These joints are generally kept open during the construction period and they are later grouted to form a monolithic structure, thus hyper-static, allowing stress transfer from one block to the other and mobilising arch effects [106] [48].

This implies that the changes in temperature with respect to that at the time of grouting generate

thermal stresses. The correct estimation of the reference temperature *(T_{ref})* (also called, zero, closing or grouting temperature) is thus essential to assess the stress field of the structure. Nonetheless, many authors often use a rough estimation of the reference temperature, which is constant for the whole dam body [6, 95], or they only assign different values to individual arches if the concrete temperature is assumed to be variable along the vertical axis [68, 92].

For the analysis of existing dams T_{ref} can be calculated from actual data recorded by embedded thermometers in the concrete during the dam construction phase [37].

Other approaches include approximating this value as the annual or long-term average concrete temperature [59] or correlating it with the environmental temperature at the time of grouting [95].

Andersson and Seppälä [8] carried out a parametric study based on numerical modelling of a real dam assessing the effect of the variation of the thermal expansion coefficient and T_{ref}. Then they chose the combination of parameters in the model that best fitted with the response recorded by the monitoring devices.

However, relevant temperature gradients may appear in general, therefore the actual thermal field at grouting is far from homogeneous.

Santillán *et al.* [89] and Mirzaborogoz *et al.* [77] computed a heterogeneous thermal field. Both used a thermal pre-simulation of several years with transient contour conditions (yearly evolution of environmental and water temperature). As soon as the results at the end of one simulated year coincide with those at the beginning of the same year, the model is assumed to have acquired a temperature distribution unaffected by the initial temperature, which is taken as the starting condition for the simulation of the operation period. However, these studies considered neither the thermal processes associated to the construction stage of the dam, nor the true evolution of the water boundary condition (water temperature and evolution of reservoir level).

Jin *et al.* [52] stated that simplified criteria are usually employed due to the lack of an accepted procedure to compute the non-uniform temperature field. They suggested a methodology to compute the reference temperature considering the temperature field at the time of joint grouting. In this article, we further develop this approach and present a procedure for estimating the reference temperature and showcase the effect of the use of different approaches by their application to a real case study.

3 Methodology

In this section, we further analyse some specific aspects. For such purpose, we defined and performed simplified computations to assess the influence of the decisions made on the results. All are based on the same case study, which is first described. Then, the numerical model and the most critical aspects identified for the correct computation of the problem are commented.

3.1 Case study description. Baserca Dam

Baserca Dam is located in the Noguera-Ribagorzana river, on the Southern part of the Pyrenees. It is a double-curvature arch dam with a maximum height over foundation of 87 m. It features vertical joints every 15 m. The construction began on August 1980 and finished after 3 years, on November 1983. The main purpose of the dam is power generation. As such, the reservoir was partially filled during construction, for which the joints needed to be grouted in three stages, namely on 1982-05-15 for the lower 36 m of the dam body, on 1983-05-15 for an additional height of 18 m and on 1984-05-15 for the upper part. The dam is thus an interesting benchmark to analyse the effect of some of the complex aspects involved in the computation of thermo-mechanical response of concrete arch dams.

The geometry of the cantilevers is such that they tend to deform in the upstream direction due to self-weight, resulting in joint opening and preventing interaction among the blocks [7]. Therefore, stresses due to self-weight can be computed assuming independent blocks.

In some areas of the dam body, the concrete temperature at early stages was controlled by means of cooling pipes. Water was injected at 8 ℃ until no change in temperature was registered in the outflow. However, no accurate information is available as to consider this effect in the numerical model.

Metallic formworks were used, as well as wood protections to prevent strong decrease in temperature during the winter season. Again, no detailed information could be gathered as for the properties of such protection, or the periods of use. As a result, formworks were also excluded from the analysis.

The lifts featured 2-m thickness and were vibrated in 4 sub-lifts of 0.5 m. Concrete with dry consistency was employed, with a water-cement ratio of 0.5.

We used the available records for the evolution of the reservoir level and the air temperature, shown in Figure 1.

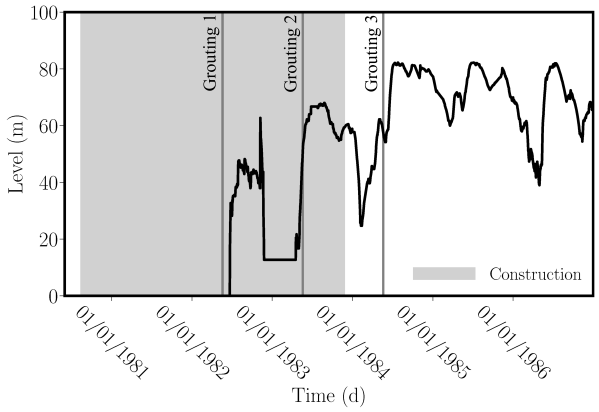

(a) Water level.

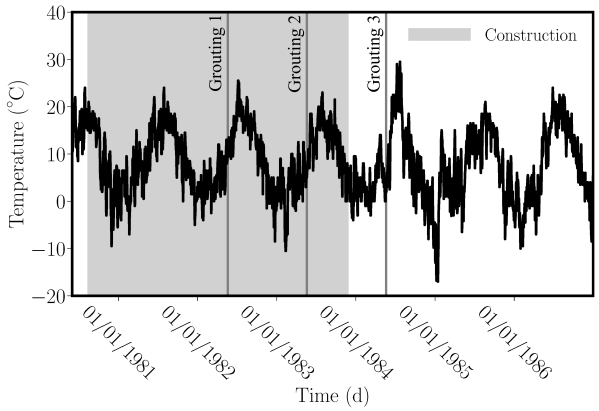

(b) Air temperature.

Fig. 1 Evolution of the reservoir level and air temperature at the dam site.

No additional information was available for the concrete properties. Therefore, we used conventional values for the material parameters and an adiabatic model for the generation of hydration heat with eq. (10). As for the placing temperature, we applied eq. (5) to consider the actual daily temperature.

The period considered for the construction process comprised from the start of construction on 1980-07-31 until 1984-30-05, i.e., 15 days after the last stage of joint grouting. This results in 1400 days of simulation. The mesh required to model each lift independently was formed by tetrahedra with an average edge length of 1 m to ensure at least 2 elements for each lift, as well as three elements in the upstream-downstream direction. For the foundation, we used increasing size until 25 m.

According to available data, the water temperature ranges from 5 ℃ to 16 ℃. It can be considered constant in winter, with around 5 ℃, and variable in depth with values oscillating from 8 ℃ to 16 ℃ in summer. These temperatures are in accordance with those suggested by Pérez Catellanos and Martínez for non-stratified reservoirs in the location of the Baserca Dam [82].

As mentioned in Section 2.4, different approaches can be used to calculate the temperature of the water, being the Bofang formula one of the most popular ones.

Some thermometer data are available for Baserca dam, so the results of the application of the Bofang formula were compared to those records (Fig. 2). It was verified that in this case the aforementioned formula overestimates the temperature in winter, while it clearly underestimates it in summer, especially near the surface. We thus chose to consider the observed data to assign the boundary condition to the wetted surfaces: the temperature recorded at the lowest location was assigned to the lower part, and the average of the remaining measures is taken for the upper area. The result of this assumption is also plotted in Fig. 2.

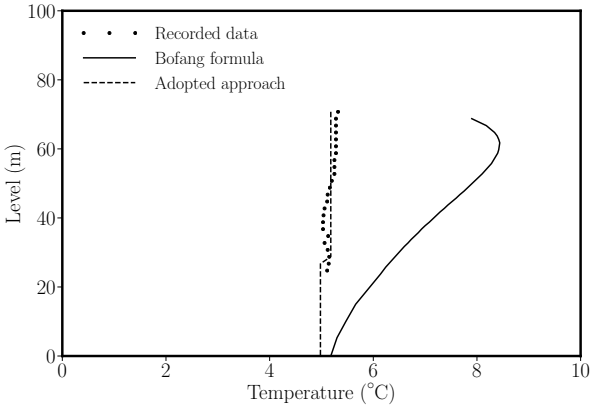

(a) Winter example (18/11/2004).

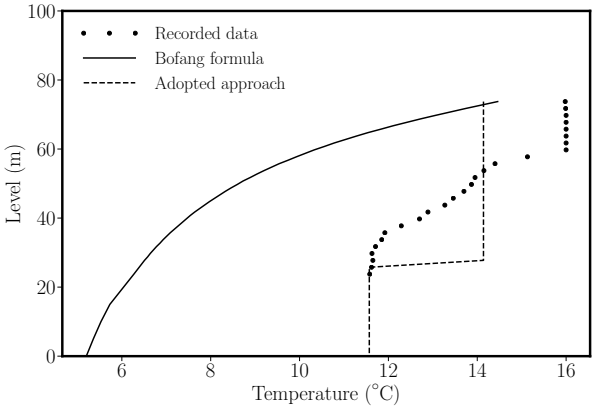

(b) Summer example (3/8/2005).

Fig. 2 Comparison of water temperature recorded at the dam site, Bofang formula and adopted approach.

The following criteria were adopted for the thermal boundary conditions:

- The actual construction process was considered according to the available information. This implies updating the boundary conditions at every time step, to account for the change in geometry and reservoir level: the surfaces in contact with air are identified to apply the heat flux condition, while the temperature is imposed on those surfaces that are in contact with the water in the reservoir. This process needs to be performed not only in the newly activated parts, but also in the previously built elements, since surfaces in contact with air may be covered with the new concrete lift in subsequent time steps.
- The placement temperature was calculated from eq. (5).
- The temperature in the wetted upstream face was set to be equal to that of the water. The actual recorded evolution of the reservoir level was taken into account. This is a relevant effect in these cases, since the reservoir was partially filled during construction in different periods, thus affecting the temperature evolution during construction.
- A heat flux condition was applied in the dry areas, both for the upstream part above water level and for the whole downstream face. The daily mean temperature was increased in 3 ℃ (to consider the effect of short wave radiation), in accordance with the estimate proposed by Pérez Catellanos and Martínez [82] for dams with Southern orientation and low wind in the Southern side of the Pyrenees.
- No other thermal effect was considered (e.g. shadows).

The material parameters used in the computations are presented in Table 5. The maximum temperature reach (T_{max}) and the parameter defining the heat generation rate (α) in the adiabatic formulation are not assigned to the ground.

Table 5 Material properties adopted for the case study.

Material property	Ground	Concrete
Density [kg/m^3]	3000	2400
Young modulus [GPa]	49	30
Poisson ratio [−]	0.25	0.20
Thermal expansion [1/℃]	10^{-5}	10^{-5}
Conductivity [W/(m · ℃)]	2.2	2.5
Specific heat [J/(kg · ℃)]	950	982
Convection coef. [W/(m^2 · ℃)]	15	15
Max. adiab. temp. rise [℃]	-	21
α [−]	-	$1.2 \cdot 10^{-5}$

3.2 Numerical model

The governing equations of the problem described in section 2.1 are approached with a one-way coupling strategy. Eq. (1) is solved first, and then the resulting temperature field T is used in the solution of eq. (3) through the constitutive model of the solid. In this case, a thermo-elastic constitutive relation was considered between the stresses and the strains:

$$\sigma_{ij} = D_{ijkl}\varepsilon_{kl} - \beta_{ij}(T - T_{ref}) \tag{14}$$

with D_{ijkl} being the fourth-order constitutive tensor of the material, ε_{kl} the deformation tensor, β_{ij} the thermal expansion tensor, and T_{ref} the reference temperature of the structure.

Different stabilisation techniques can be found in the literature to solve the heat transfer problem without spurious oscillations [32, 81]. In this work, we modified eq. (1) following the classical streamline upwind Petrov-Galerkin (SUPG) method [32] as it shows accurate results for diffusion-dominant problems. Eq. (3) is solved in the irreducible form after applying the standard Galerkin technique [114].

Both equations were discretised using linear tetrahedral elements with equal order interpolation for the temperature and displacement fields. The use of this typology of elements is motivated by their geometric versatility and by the fact that, using an appropriate mesh, they yield to an accurate and robust solution of the problem of interest without the need to resort to more complex formulations [20, 21].

3.3 Determination of the appropriate time step

As mentioned in Section 2.6.1, the use of an implicit Backward Euler scheme can be advantageous in our problem. This scheme is unconditionally stable, i.e., the error will become stable when approaching the steady state situation [75].

The thermal behaviour of concrete dams is far from stationary both during operation and in particular at early stages, when the hydration heat plays a relevant role and induces non-linearities that may lead to oscillations in the response of the numerical calculation [18]. This is more acute when long transient analysis are needed, since long time steps are favourable to avoid excessive computational time. It is thus interesting to analyse the effect of the time step in the results.

Since our goal is to consider the whole life cycle of the structure, there is a need to find a trade-off between enough accuracy and affordable computational time, ensuring that the whole

construction process can be considered. Our main aim was to analyse the effect of the reference temperature, rather than the thermal gradients at early stages.

We estimated the mean calculation time to solve each time step taking into account that, as the construction of the dam progresses, the number of elements is higher, and so the computational cost increases. Considering that the solver takes a mean time of about 6 minutes for every time step, the overall required time to model the construction process for different values of the time step is presented in Table 6.

Table 6 Estimated computational time for the full construction process using different time steps.

Time step (hours)	# Time steps required	Computational time (days)
1	33600	140
3	11200	46.67
6	5600	23.33
12	2800	11.67

The rate of hydration heat generation changes significantly right after concrete pouring. If an accurate analysis of the thermal gradient generated is needed, a small time step is required. We analysed the effect of using large time steps in the temperature rise underwent by concrete. For simplicity, we considered adiabatic conditions for this analysis.

We computed the temperature evolution of concrete in adiabatic conditions by integrating eq. (10) with different values of the time step. Since the heat generation decreases sharply during the first hours after pouring, an error is introduced with the time discretization if the heat generation rate at $t = t_n$ is adopted for the whole time step $[t_n - t_{n+1}]$. This is equivalent to assume that the heat rate generation at the beginning of the time step remains constant throughout the step, which results in a higher temperature. This error can be reduced if the heat generation at $t = t_{n+0.5}$ is adopted instead.

The results of discretising this formula with both approaches was compared to the adiabatic temperature, which can be computed analytically with:

$$T_{ad}(t) = T_{max}\alpha(1 - e^{-\alpha t}) \tag{15}$$

On a separated note, it should be considered that the use of large time steps in thermal problems with relatively large thermal gradients may result in convergence problems [101]. These gradients may appear in our case, since there can be high difference in temperature between pouring concrete and adjacent blocks [18].

The heat flux conditions, which are applied in the dry walls of the dam to account for the climatic effects, can also generate instabilities. In this case, the use of a large computational time step would lead to the application of an unrealistic heat flux. The reason is that while it depends on the difference between the temperature of the dam and the ambient temperature at each moment, a constant flux is applied throughout the entire step which only depends on the initial temperature.

To verify these issues, we analysed several test cases with different time steps: 1, 3, 6 and 12 hours. We used a simplified, although realistic, domain. It is based on the case study, and comprises the bottom part of 5 central cantilevers, up to 40 m (4 m above the first stage of joint grouting). Figure 3 shows the geometry of the simplified domain, together with the locations where the temperature was recorded. They were taken at intermediate thickness in different lifts, except T_1, at the bottom, and T_3, at the top of the second lift. The latter is interesting because it remained uncovered for relatively long time.

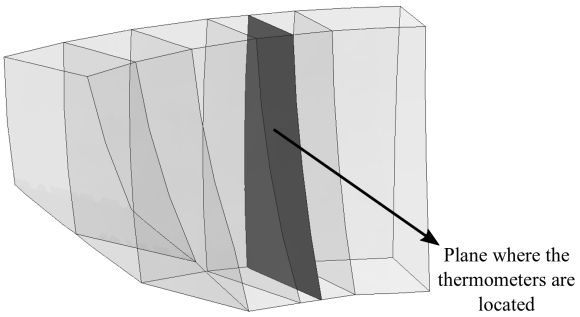

(a) Geometry of the simplified domain.

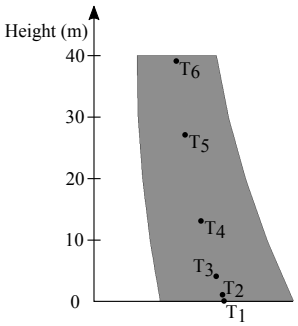

(b) Thermometers location.

Fig. 3 Geometry of the simplified domain and location of the thermometers.

3.4 Computational domain

In this study, we compared several configurations of the numerical model for the dam and the foundation with different computational domains and thermal boundary conditions. As a reference model, we took the simplified 6-h case from the previous section without foundation (see Figure 3), and two different boundary conditions for the dam-foundation interface: adiabatic and imposed temperature. For the latter, we took the ground temperature at the moment of concrete placement.

Two additional options were simulated including an explicit modelling of the foundation: with a reduced ground portion of 10 m depth, and with the conventional dimensions for structural analyses (foundation domain larger than two heights of the dam in depth, upstream and downstream directions and more than half length of the dam on the left and right sides). In both cases with explicit foundation, a constant temperature was imposed at the bottom surface of the domain equal to the annual mean ambient temperature [49]. The rest of the surfaces (vertical cuts of the domain) were considered adiabatic.

The different computational domains are depicted in Figure 4, where the number of nodes and elements are shown. It can be noticed that there is a relevant increase in computational burden even though a larger mesh size was used for the foundation.

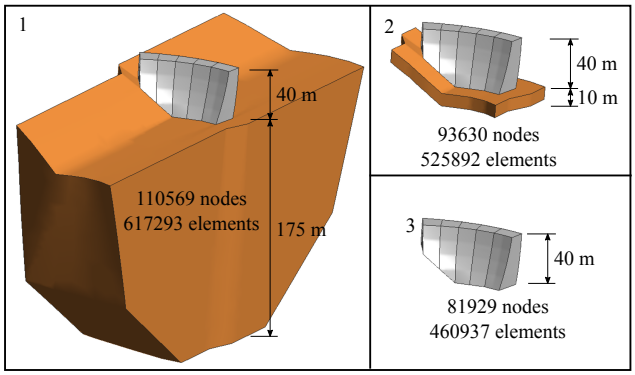

Fig. 4 Computational domain of the simplified geometry with the conventional ground dimensions for structural analysis (1), with a reduced ground portion of 10 m depth (2) and without foundation (3).

The comparative analysis was carried out by monitoring the temperature of the same points shown in previous section (Figure 3) located at different heights inside the dam. The objective of this analysis is to evaluate the influence of the foundation on the temperature reached in the dam depending on the criteria used to simulate the dam-foundation interaction.

3.5 Effect of the reference temperature on the stress field during operation

Most of the technical reference documents and real case studies analysed here propose a fixed value of T_{ref} for the whole dam [6, 59, 95] or different values linked to sub-regions of the dam as a function of the elevation [48, 92, 106]. Although it has been barely applied, some documents mention the convenience of using a non-uniform temperature field rather than a single value due to the differences between the inner part of the dam and the faces [52, 86]. However, the few studies where a distributed reference temperature field was computed did not consider the thermal processes involved during the construction stage [77, 89].

There is thus an agreement on the high relevance of the accurate determination of the reference temperature in the stress field during operation, but simplified approaches are still applied, and the effect of such assumptions has not been assessed. This is one of the main objectives of our work, for which we compared the results of different approaches to compute T_{ref}:

1. As a constant value equal to 7.24 ℃, i.e., the average temperature by the grouting time (in May).
2. As the thermal field obtained from a simplified transient calculation: the reservoir was considered empty and a thermal model is run from 1980-06-01 until 1984-05-15 with the same assumptions of the detailed model, except for the construction process and the hydration heat.
3. As the thermal field at the date of grouting of each subdomain, resulting from the detailed transient thermal analysis.

The implementation of the detailed computational procedure required the creation of T_{ref} as a *nodal variable* (each node in the model has a specific value of the T_{ref} assigned). Since we neglect thermal stresses before joint grouting, this variable is de-activated at the initial time step of the simulation ($t = t_0$). A different grouting time $t_{grout,k}$ is assigned to each subdomain k. When $t = t_{grout,k}$, the resulting temperature T_i obtained from the thermal problem is taken as T_{ref} for subdomain k. Thermal stresses are computed for subsequent time steps on such subdomain. The simulation of the construction process continues until the end of the construction,

with the same procedure for assigning T_{ref} to the remaining subdomains. Once the grouting is completed, thermal stresses are computed in the whole dam body. Figure 5 summarizes the main steps involved in the development of the reference temperature in this study.

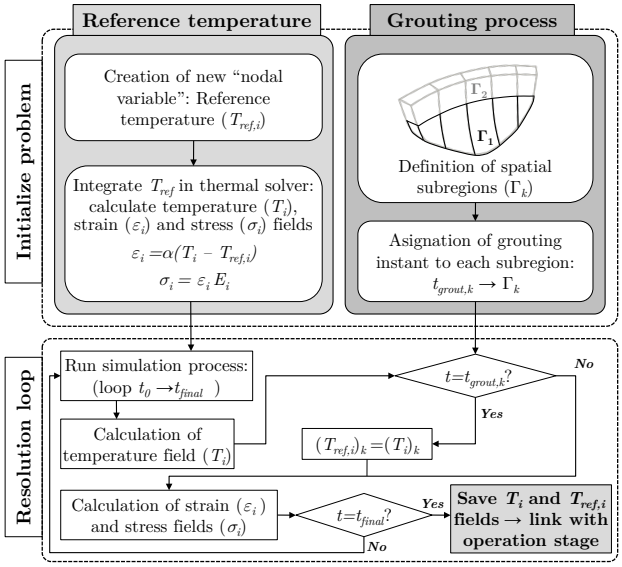

Fig. 5 Flux diagram of processes developed involving reference temperature.

3.6 Link between construction and operation stages

It was already mentioned that the calculation of the construction process requires a fine mesh to consider each lift. By contrast, in the exploitation phase, a thicker mesh may be admissible, especially in height (it is advisable to maintain at least 3 elements along the dam thickness). It is common to calculate the state of the dam at the end of the construction as a combination of self-weight, hydrostatic load and temperature. In addition, it should be remembered that self-weight displacements at the end of construction are disregarded, as in practice they are corrected during construction. Regardless of the criteria used for each process, it must be possible to combine them. A functionality has been developed that allows the results of different calculations to be combined with different geometries, meshes and time steps. This allows for example to calculate the self-weight on a model with the separated cantilevers, and combine the result with that of a monolithic thermal model.

In addition to the thermal variables required for the combination of the construction and operation stages (concrete temperature at the end of construction and reference temperature), mechanical stresses due to self-weight and hydrostatic load also need to be accounted for to have a realistic estimate of the stress field during operation.

The stresses due to self-weight are computed by superimposing the results of three mechanical models to account for the staged grouting, as described in Figure 6. Displacements are neglected.

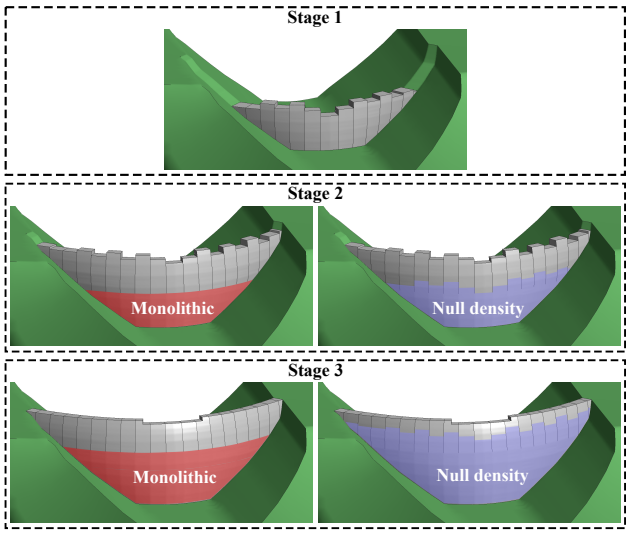

Fig. 6 Models used to compute self-weight to account for the staged grouting. Stage 1 is calculated with separated cantilevers. In stages 2 and 3, the part already grouted is considered monolithic, while the cantilevers not yet grouted are assumed to be independent. The stresses of the previous stages are added in the part already calculated where null density is assigned.

On a different calculation, the complete construction process is modelled to obtain T_{ref} as the temperature field at the time of grouting for each subdomain.

A separated thermo-mechanical model is later used for the computation of the dam response during operation. The thermal field at the end of construction is taken as the initial temperature. The thermal stresses are computed using the T_{ref} obtained from the detailed model of the construction process. The stresses due to self-weight are finally added to the resulting stresses due to hydrostatic load.

The computation was performed using an in-house specific application for thermo-mechanical analysis of the entire life cycle of concrete dams, with specific features for double-curvature arch dams. It is based on the open-source framework Kratos Multiphysics [29] and solves both the thermal and mechanical parts of the problem.

The main ingredients of the process can be summarised as follows:

1. The construction process can be realistically considered, since the external surfaces of each cantilever are identified as the construction progresses, and the appropriate boundary conditions are applied.
2. Both the construction and the operation periods can be analysed in a unified framework.
3. It is integrated with an assistant for generating the geometry and mesh of double-curvature arch dams [107], which facilitates the whole design and analysis process.
4. The reference temperature can be taken from different time steps of the construction phase, and assigned to different areas of the dam body. This allows reproducing the staged joint grouting.
5. Different degrees of detail can be adopted for the involved phenomena. This allows for example running long transient analysis with fine meshes at a moderate computational cost. For that purpose, specific functionalities were implemented to run different calculations with appropriate time steps and mesh sizes, even over different domains, which can be later combined to compute the overall solution.

A transient thermo-mechanical analysis was run from 1984-01-01 until 1986-12-31 with the different approaches described in the previous section to account for T_{ref}. The results in terms of stress field and displacements were recorded and analysed, with focus on two dates, representative of full reservoir in winter (1985-02-01), and the lowest reservoir level registered in that period (55 m, on 1986-11-10).

4 Results

4.1 Effect of the time step

The temperature evolution of concrete in adiabatic conditions obtained from the integration of eq. (10) using the heat generation rate at the beginning ($t = t_n$) and in the middle ($t = t_{n+0.5}$) of the time step is shown in Fig. 7. These results are compared to the adiabatic analytical solution obtained by applying eq. (15).

Figure 8 presents the error obtained with each discretised formulation with respect to the analytical solution.

The results show that using the heat generation rate at $t_{n+0.5}$ is beneficial for any value of the time step, since the difference with respect to the analytical solution is negligible after three days. The use of the value at t_n results in an important error, which is greater with larger time steps.

Although the error depends on the concrete properties and would be different in case a non-adiabatic formulation is used, this analysis can be useful to obtain a first approximation of the accuracy to be expected when large time steps are adopted.

Since our main interest is the accurate estimation of the reference temperature, other sources of instabilities should be taken into account such as the large thermal gradients between elements and heat flux boundary conditions. To analyse these issues we computed the simplified geometry cases presented in section 3.3 with the heat generation rate at time $t_{n+0.5}$. The temperature obtained at the set of points shown in Figure 3 was analysed.

Figure 9 shows the temperature of each point over time for different time steps: 12 h, 6 h, 3 h and 1 h. The maximum difference between using $\Delta t = 12$ h and $\Delta t = 1$ h is about 2 ℃ and 0.5 ℃ in thermometers 4 and 5 respectively. On the other hand, the differences in the long term temperature among models with $\Delta t = 6$ h or lower are negligible.

Thermometer 3 is located at the top of the second lift and its results are interesting because it remained uncovered for a long time before the upper lift was poured. The results shown in Figure 9 indicate that the long-term temperature is independent of the chosen time step. However, relevant differences are observed in the short term, before the third lift is placed.

A close analysis of the temperature evolution in thermometer 3 (Figure 10) reveals relevant oscillations due to changes in ambient temperature, which are more acute for large time steps. This result is unrealistic, since it comes from the application of a constant heat flux throughout the entire time step. Differences are minor for $\Delta t = 6$ h or lower. In view of this results, $\Delta t = 6$ h was used for the full analysis.

4.2 Computational domain

The results of the approaches tested for the computational domain are shown in Figure 11. They show that the application of adiabatic boundary conditions leads to lower energy dissipation and higher temperature in the lower area.

The imposition of a fixed temperature (in this case the mean annual temperature in the dam location), leads to errors at the lower blocks during the initial steps, which decrease with time.

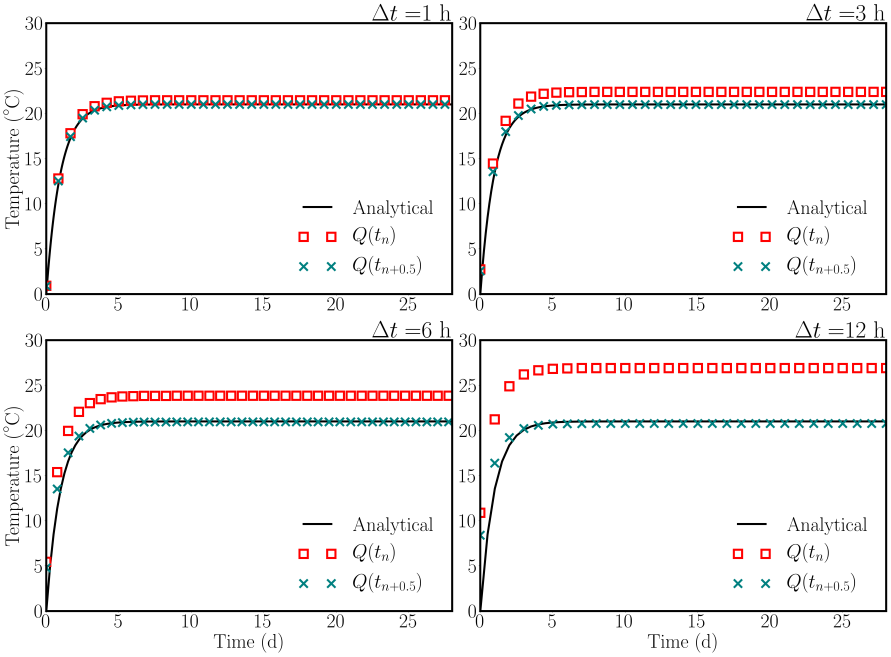

Fig. 7 Evolution of temperature over time: analytical solution and discretised formulations with different time steps.

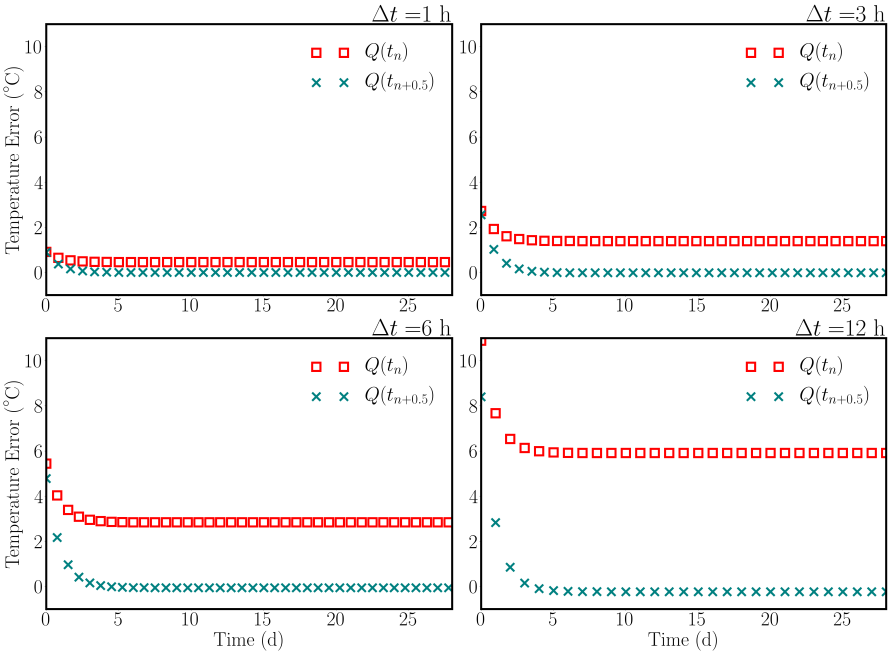

Fig. 8 Error in the calculation of the temperature for each time step with the two discretised formulations.

The comparison between the four options considered clearly shows that using a limited foundation is advantageous, since the difference in temperature in the dam body is negligible with respect to case with large foundation, with lower computational cost. On the other hand, removing the foundation has an effect in the lower part of the cantilevers. If the computational cost requires excluding the ground, the results suggest that the average annual temperature should be applied instead of an adiabatic boundary condition.

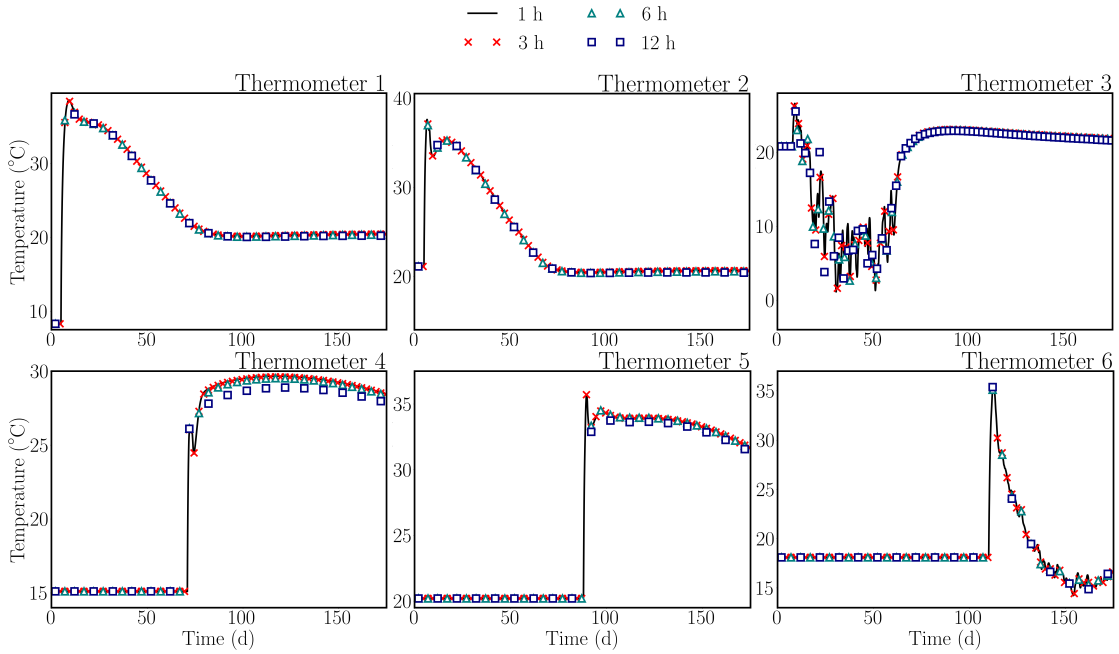

Fig. 9 Temperature evolution in the thermometers considered (see Figure 3) for different values of the time step.

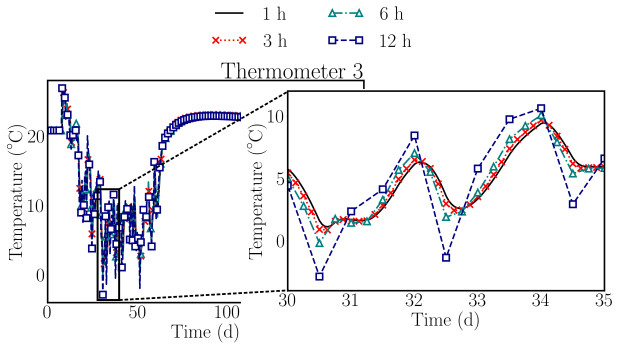

Fig. 10 Detail of the temperature evolution in thermometer 3 while in contact with air.

4.3 Reference temperature

Figure 12 shows the resulting reference temperature in the three situations considered. In the first one, the average temperature at the time of the three stages of grouting (7.24 ℃) is considered as T_{ref} for the whole dam body.

The simplified process results in a reference temperature in most of the dam body around 3 ℃ higher than the average air temperature in May. This is explained by the unusually high ambient temperature during the weeks before the third grouting. By contrast, some cold days right before the end of construction resulted in a thin area with lower values for T_{ref}.

The results from the detailed calculation show the different conditions in each grouting stage. The outer area features different temperature, with similar thickness to that from the simplified transient analysis. The upstream face shows the effect of the water temperature and the consideration of the reservoir level.

As for the internal part, a bulb of relevant size can be seen in the bottom part with T_{ref} close to 20 ℃. This result clearly shows that the hydration heat had not been dissipated at the time of grouting.

It should be reminded that neither model is representative of the actual performance of the dam. In particular, the cooling pipes were not considered in the detailed model, which obviously contributed to dissipating the hydration heat. This result confirms the need for such measures to control temperature rise.

4.4 Stress state during operation

The computation procedure for all three cases is identical for the operation phase (transient thermo-mechanical), and so is the thermal field. However, differences in the computation of T_{ref} result in different values of displacements and thermal stresses during operation.

Figure 13 shows results for 1985-01-02, with reservoir level at 94 %. The mean air temperature was −13 ℃ and low values were also registered in the

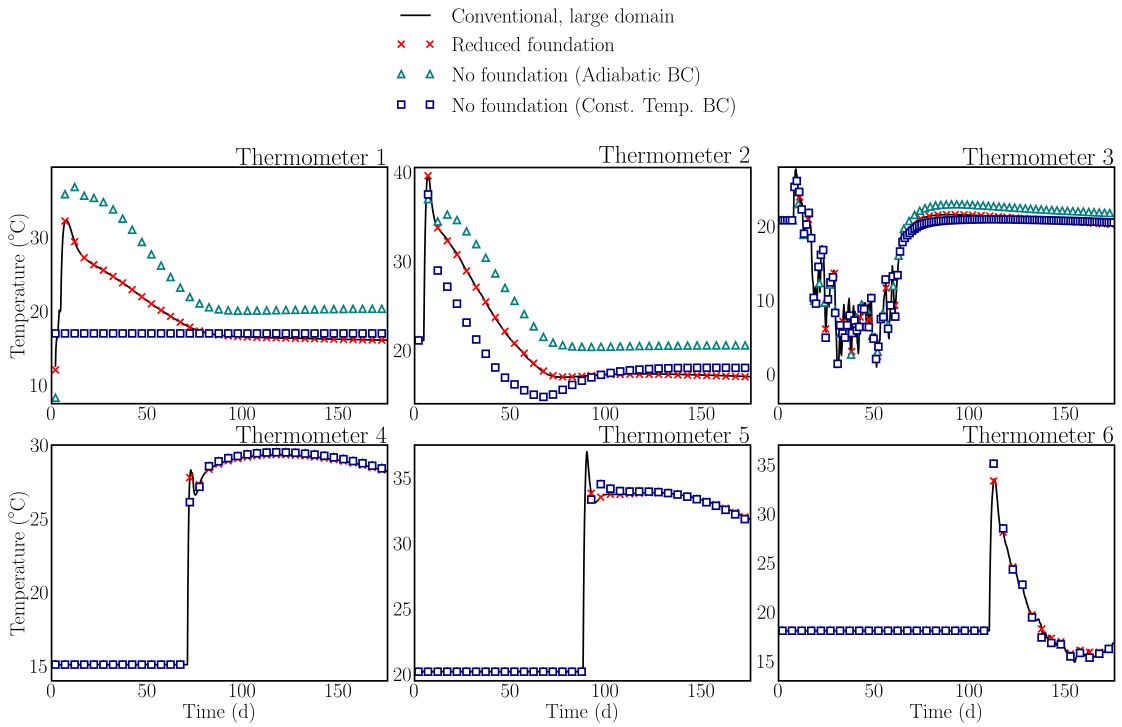

Fig. 11 Effect of the foundation on the temperature evolution in different control points (see location in Figure 3)

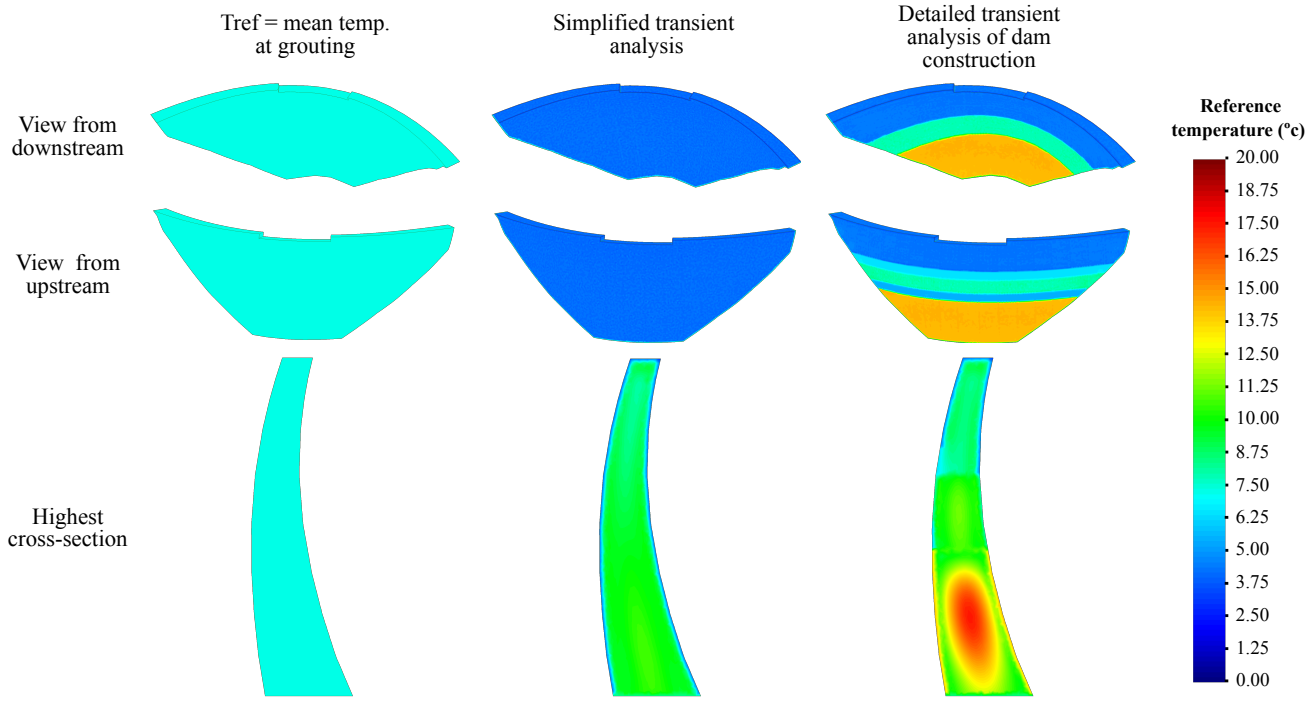

Fig. 12 Reference temperature obtained with the approaches considered. Views of the upstream and downstream faces, as well as cross section of the highest cantilever.

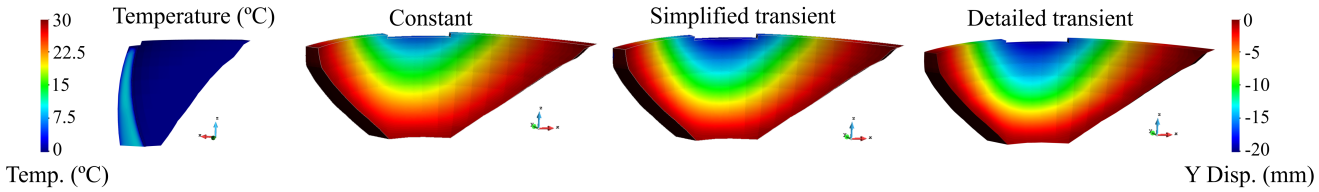

Fig. 13 Results for temperature (left) and Y displacements on 1985-01-02.

previous weeks. This results in low temperature in the dam body and in particular in the outer areas. As a consequence, both the thermal and the hydrostatic effect generated deformations toward downstream.

The thermal deformation is computed as a function of the deviation of the actual temperature from T_{ref}. Therefore, the resulting displacement field varies among procedures. Results are similar between the simplified transient and the detailed approach, but the maximum displacement is 15 % lower if the first method is used. This may have relevant consequences when calibrating numerical models with monitoring data. The displacements measured at pendula are often used for such purpose: once a numerical model correctly reproduces the observed displacements, it is used to analyze the stresses. If the contribution of the thermal effect to the deformations is not correctly reproduced, decisions made on the basis of the corresponding stress field can be misleading.

The stress field is also different for each situation considered. For this load combination, both the hydrostatic load and the temperature decrease tend to generate tensile stresses at the upstream toe. Such tensile stress is obtained with all three approaches (Fig. 14a), although both the maximum value and the affected area are different. This can be better observed in Fig. 14b, where areas with tensile stresses greater than 1 MPa are highlighted.

Tensile stresses are also registered in superficial regions, both in the upstream and downstream faces. Their magnitude is low, except for very localized areas close to the foundation. The distribution is nonetheless highly different among procedures. This may be relevant when estimating the magnitude and areas affected by superficial cracking.

The main difference is nonetheless the bulb of tensile stresses obtained with the detailed analysis. This is the direct result of the non-dissipated hydration heat that was reflected in high T_{ref} on such region. Again, the need for adopting measures for refrigerating the poured concrete is verified. Such result may be useful in the design stage, when the construction plan and means are to be determined.

Similar conclusions can be drawn from the results on 1986-11-10, although the magnitude of displacements and temperatures is obviously different. Figure 15 shows the thermal and the Y-displacement fields. In this case, with lower hydrostatic load and higher temperature, the crest deforms in the upstream direction, with lower value. However, there is still a relevant difference between the maximum displacement when constant T_{ref} is applied (10 mm) with respect to other approaches (12 mm). Again, such deviation may be essential for model calibration.

Although superficial tensile stresses are smaller and so is the affected area, the location is again strongly different (Figure 15). Even in this favourable load combination, positive stresses are registered in the lower inner area of the central blocks. This is a further verification of the need for refrigerating means.

5 Summary and Conclusions

In this work, the most noticeable aspects involved in the numerical modelling of the thermo-mechanical response of arch dams were assessed, with special attention paid on the construction process and the determination of the reference temperature. A deep literature review was performed, resulting in a compilation of relevant information on the criteria used by different authors with regard to the model generation, such as boundary conditions, computational domain, or time integration. Also, the parameters adopted for different case studies were presented. This can be useful as a reference for future works, in case some information is missing regarding for instance the concrete properties.

In addition, some particular points were specifically treated in this work, namely the time step, the computational domain and the approach to compute the reference temperature.

The conclusions obtained from the bibliographic review and from the specific studies performed in this work are summarised in Table 7.

The degree of detail to be used for each element involved in the numerical modelling of arch dams depends mainly on the objective of the calculation

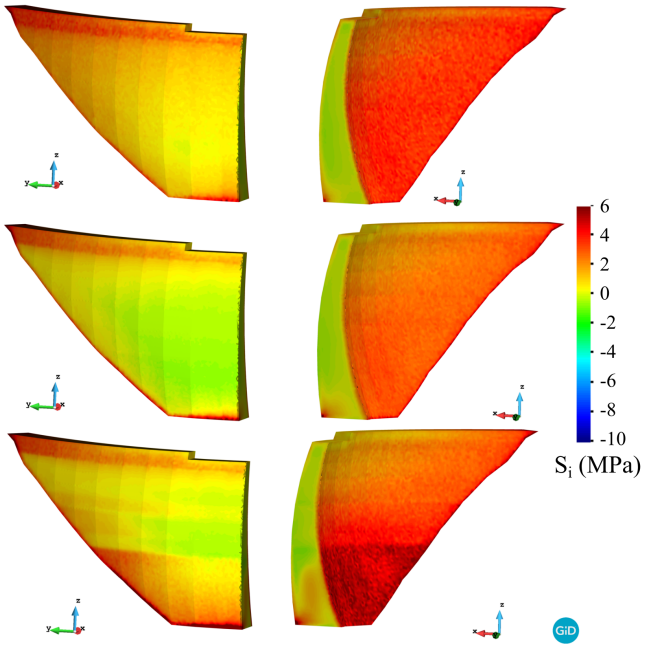

(a) Maximum principal stress.

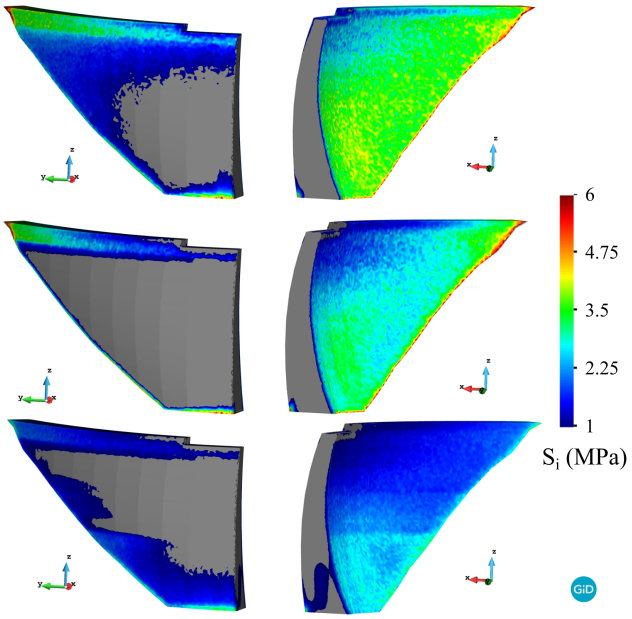

(b) Areas with tensile stress higher than 1 MPa.

Fig. 14 Results for 1985-01-02. Hydrostatic load: 94 %. From top to bottom: Constant temperature, simplified transient and detailed transient.

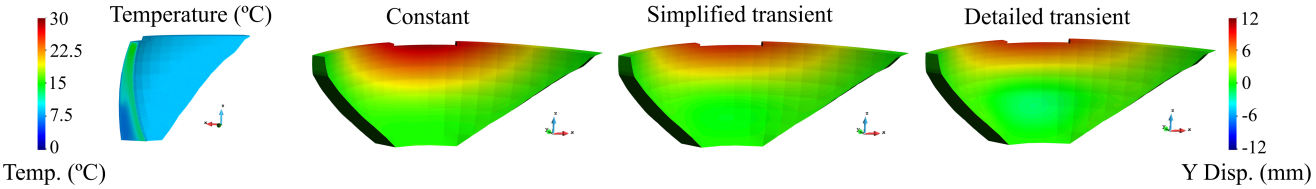

Fig. 15 Results for temperature (left) and Y displacements on 1986-11-10.

(design or verification), the information available and the characteristics of the dam. Whatever the case, the results of this work show the relevance of an adequate computation of the reference temperature on the stress field during operation. The use of an unrealistic estimate may result in inaccurate results for the stress state of the dam, and lead to inadequate decisions in terms of maintenance and safety.

Acknowledgements This work was partially funded by the Spanish Ministry of Science, Innovation and Universities through the project TRISTAN (RTI2018-094785-B-I00). The authors also acknowledge financial support from the Spanish Ministry of Economy and Competitiveness, through the "Severo Ochoa Programme for Centres of Excellence in R&D" (CEX2018-000797-S), and from the Generalitat de Catalunya through the CERCA Program.

Conflict of interest

On behalf of all authors, the corresponding author states that there is no conflict of interest.

References

1. Abdulrazeg, A.A., Noorzaei, J., Jaafar, M.S., Khanehzaei, P., Mohamed, T.A.: Thermal and structural analysis of rcc double-curvature arch dam. Journal of Civil Engineering and Management **20**(3), 434–445 (2014)
2. ACI Committee 207: Report on thermal and volume change effects on cracking of mass concrete. Tech. rep., American Concrete Institute (2007)
3. Agulló, L., Mirambell, E., Aguado, A.: A model for the analysis of concrete dams due to environmental thermal effects. International Journal of Numerical Methods for Heat & Fluid Flow **6**(4), 25–36 (1996)
4. Agulló, L., Mirambell, E., Aguado, A.: Comportamiento térmico de presas de hormigón frente a la acción térmica ambiental. Revista de Obras Públicas **144**(3362), 19–28 (1997)

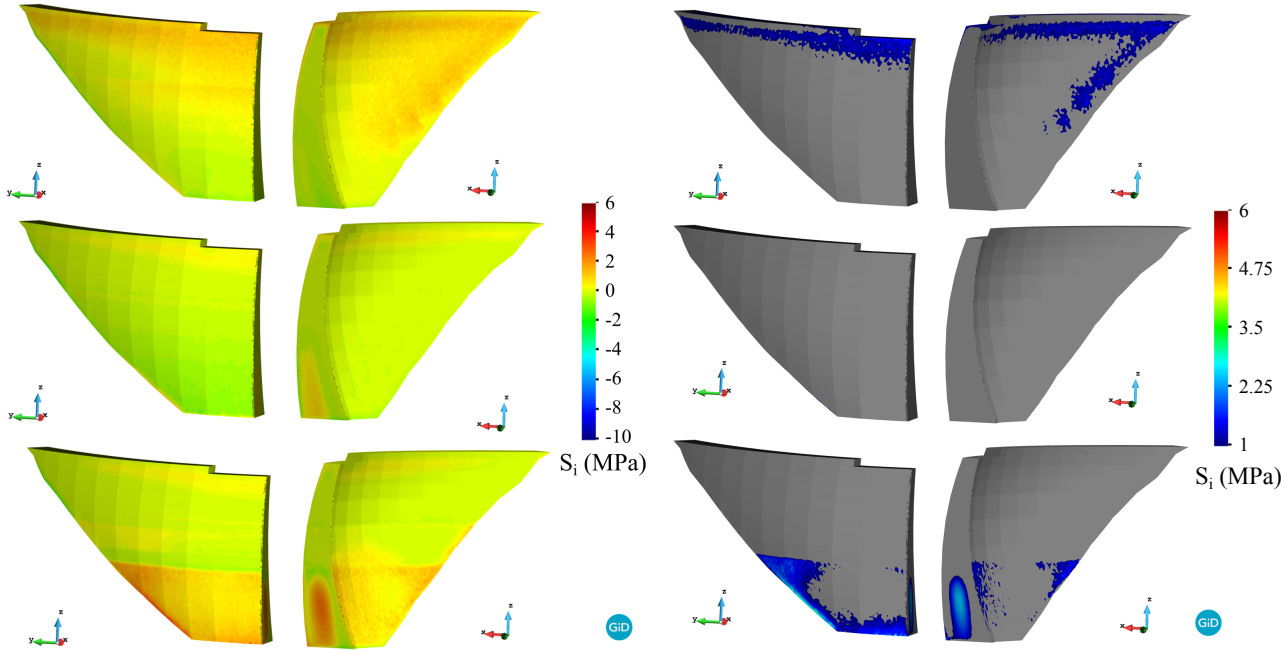

(a) Maximum principal stress.

(b) Areas with tensile stress higher than 1 MPa.

Fig. 16 Results for 1986-11-10. Hydrostatic load: 68 %. From top to bottom: Constant temperature, simplified transient and detailed transient.

5. Akbari, J., Ahmadi, M.T., Moharrami, H.: Advances in concrete arch dams shape optimization. Applied Mathematical Modelling **35**(7), 3316–3333 (2011)
6. Alembagheri, M.: A study on structural safety of concrete arch dams during construction and operation phases. Geotechnical and Geological Engineering **37**, 571–591 (2018)
7. Álvarez Martínez, A., Buil Sanz, J.M., Herrero Pérez, E.: Salto de moralets. presa de barseca y de llauset. Revista de Obras Públicas **132**, 353–368 (1985)
8. Andersson, O., Seppälä, M.: Verification of the response of a concrete arch dam subjected to seasonal temperature variations. Master thesis, Royal Institute of Technology (KTH), Stockholm, Sweden (2015)
9. de Araújo, J., Awruch, A.M.: Cracking safety evaluation on gravity concrete dams during the construction phase. Computers & structures **66**(1), 93–104 (1998)
10. Ardito, R., Maier, G., Massalongo, G.: Diagnostic analysis of concrete dams based on seasonal hydrostatic loading. Engineering Structures **30**(11), 3176–3185 (2008)
11. Azenha, M.: Numerical simulation of the structural behaviour of concrete since its early ages. Ph.D. thesis, Tese de Doutorado. Faculdade de Engenharia da Universidade do Porto–FEUP. Porto (2009)
12. Azenha, M., Lameiras, R., de Sousa, C., Barros, J.: Application of air cooled pipes for reduction of early age cracking risk in a massive rc wall. Engineering Structures **62**, 148–163 (2014)
13. Azmi, M., Paultre, P.: Three-dimensional analysis of concrete dams including contraction joint non-linearity. Engineering Structures **24**(6), 757–771 (2002)
14. Bayagoob, K.H., Bamaga, S.O.: Construction of Roller Compacted Concrete Dams in Hot Arid Regions. Materials **12**(19) (2019)
15. Belmokre, A., Mihoubi, M.K., Santillán, D.: Analysis of Dam Behavior by Statistical Models: Application of the Random Forest Approach. KSCE Journal of Civil Engineering **23**(11), 4800–4811 (2019)
16. Briffaut, M., Benboudjema, F., Torrenti, J.M., Nahas, G.: Effects of early-age thermal behaviour on damage risks in massive concrete structures. European Journal of Environmental and Civil Engineering **16**(5), 589–605 (2012)
17. Brown, A.I., Marco, S.M.: Introduction to heat transfer. Third edition. McGraw-Hill (1958)
18. Castilho, E., Schclar, N., Tiago, C., Farinha, M.L.B.: Fea model for the simulation of the hydration process and temperature evolution during the concreting of an arch dam. Engineering Structures **174**, 165–177 (2018)
19. Castilho, E.M., Leitão, N.S., Tiago, C.: Thermal analysis of concrete dams during construction phase. In: Second International Dam World Conference (2015)
20. Cervera, M., Chiumenti, M., Codina, R.: Mixed stabilized finite element methods in nonlinear solid mechanics: Part I: Formulation. Computer Methods in Applied Mechanics and Engineering **199**(37), 2559–2570 (2010)
21. Cervera, M., Chiumenti, M., Valverde, Q., Agelet de Saracibar, C.: Mixed linear/linear simplicial elements for incompressible elasticity and plasticity. Computer Methods in Applied Mechanics and Engineering **192**(49), 5249–5263 (2003)
22. Cervera, M., Garcia, J.: Simulación numérica del comportamiento termo-mecánico de presas de hcr parte ii: Aplicación a la presa de rialb. Revista internacional de métodos numéricos para cálculo y diseño en ingeniería **18**(1), 95–110 (2002)
23. Cervera, M., Oliver, J., Prato, T.: Thermo-chemo-mechanical model for concrete. i: Hydration and ag-

Table 7 Summary of conclusions and recommendations for each topic involved.

Topic	Conclusions/recommendations
Governing equations	Conventional thermo-mechanical equations, one-way coupling.
Self weight	Monolithic is not recommended. Independent cantilevers is a good approximation in general. Construction process needs to be considered in case of staged grouting. Non-linear joint elements only in singular cases, since can result in convergence issues and uncertainty in results.
Placement temperature	Depends on the air temperature, storage conditions and manipulation process. Effect of ambient temperature can be considered with the empirical approximation proposed by Briffaut [16].
Hydration heat	Non-adiabatic approach is more realistic. However, it requires detailed knowledge of the environmental conditions, and a complex model. Adiabatic approach is a good estimate for the dam body, except for the external surfaces. Experimental data is necessary in both cases to determine the parameters.
Cooling	Has a relevant impact on the reference temperature. Can be estimated with simplified approaches. Detailed analysis including water flow and heat exchange with concrete are recommended for optimization of the cooling process in relevant projects such as super-high dams.
Formworks	Need to be considered as appropriate boundary conditions in the area of application.
Air	The effect of detailed boundary conditions was verified in different works dealing with the operation stage. However, they require very detailed information on environmental conditions, such as wind speed and solar radiation. Those data are difficult to acquire and apply: in the design stage, they need to be estimated. In back analysis, a comprehensive measurement system would be necessary. The estimation of the thermal field from thermometers embedded in the dam body may be a more efficient solution in that case.
Water	The water temperature should be applied as imposed boundary condition in the wetted areas, for which the variation of the reservoir level is required. During operation, the evolution of water temperature over time and in depth can be obtained from thermometers, if available. If that is not the case (design stage or absence of sensors), the Bofang formula can be useful citebofang1997prediction. However, it should be checked for the particular conditions of the site to avoid unrealistic results.
Concrete properties	They depend on the properties of the materials in the mix. They can be typically measured on site for modelling the operation stage. For design, they can be estimated from other case studies (Table 4).
Time integration	The time step should be taken as a trade-off to avoid convergence issues, to limit the overall computational time, and to achieve accuracy. Preliminary tests on the effect of the time step and estimates on the total time can be useful. The Backward Euler scheme is recommended for the time integration.
Computational domain	For the thermal problem, a reduced foundation (around 10 m depth) is enough to consider its effect on the thermal field. If only the dam body is modelled, taking an estimate of the average temperature in the dam-foundation interface as imposed temperature is more adequate than an adiabatic boundary condition.
Reference temperature	The results show the relevant effect of the reference temperature on the stress field during operation. The use of a unique value is highly unrealistic. A detailed model is recommended for determining T_{ref}, especially when grouting is performed in different stages. Taking rough estimates may lead to relevant errors in the stress field and to wrong model calibration, which in turn may result in inadequate decisions regarding dam safety.

ing. Journal of engineering mechanics **125**(9), 1018–1027 (1999)
24. Cervera, M., Oliver, J., Prato, T.: Thermo-chemo-mechanical model for concrete. ii: Damage and creep. Journal of engineering mechanics **125**(9), 1028–1039 (1999)
25. Cervera Miguel, Oliver Javier, Prato Tomás: Simulation of Construction of RCC Dams. I: Temperature and Aging. Journal of Structural Engineering **126**(9), 1053–1061 (2000)
26. Chen, S.h., Su, P., Shahrour, I.: Composite element algorithm for the thermal analysis of mass concrete: simulation of cooling pipes. International Journal of Numerical Methods for Heat & Fluid Flow **21**(4), 434–447 (2011)

27. Conceição, J., Faria, R., Azenha, M.: Thermo-mechanical analysis of an arch dam monolith during construction. In: Proc. Congress on Numerical Methods in Engineering (CMN 2017). International Centre for Numerical Methods in Engineering (CIMNE) (2017)
28. Conceição, J., Faria, R., Azenha, M., Miranda, M.: A new method based on equivalent surfaces for simulation of the post-cooling in concrete arch dams during construction. Engineering Structures p. 109976 (2019)
29. Dadvand, P., Rossi, R., Oñate, E.: An object-oriented environment for developing finite element codes for multi-disciplinary applications. Archives of computational methods in engineering **17**(3), 253–297 (2010)
30. Daoud, M., Galanis, N., Ballivy, G.: Calculation of the periodic temperature field in a concrete dam. Canadian Journal of Civil Engineering **24**(5), 772–784 (1997)
31. de-Pouplana, I., Oñate, E.: A FIC-based stabilized mixed finite element method with equal order interpolation for solid–pore fluid interaction problems. International Journal for Numerical and Analytical Methods in Geomechanics **41**(1), 110–134 (2017)
32. Donea, J., Huerta, A.: Finite element methods for flow problems. John Wiley & Sons (2003)
33. Duffie, J.A.: Solar Engineering of Thermal Processes, edición: 4th edition edn. John Wiley & Sons, Hoboken (2013)
34. Enzell, J., Tollsten, M.: Thermal cracking of a concrete arch dam due to seasonal temperature variations. Master's thesis, Royal Institute of Technology (KTH) (2017)
35. Escuder, I., Serrano-Lombillo, A., Vilaplana, A.: Initial strain and stress development in a thin arch dam considering realistic construction sequence. In: Proceedings of the Tenth ICOLD Benchmark Workshop on Numerical Analysis of Dams. Paris, France (2009)
36. Feng, J., Wei, H., Pan, J., Jian, Y., Wang, J., Zhang, C.: Comparative study procedure for the safety evaluation of high arch dams. Computers and Geotechnics **38**(3), 306–317 (2011)
37. FERC: Engineering Guidelines for the Evaluation of Hydropower Projects, Chapter 11-Arch Dams, chap. Chapter 11-Arch Dams, pp. 1–42. Federal Energy Regulatory Commission Division (1999)
38. Goldgruber, M.: Nonlinear seismic modelling of concrete dams. Ph.D. thesis, TU Graz (2015). Austria
39. Hariri-Ardebili, M., Mirzabozorg, H.: Feasibility study of dez arch dam heightening based on nonlinear numerical analysis of existing dam. Archives of Civil Engineering **59**(1), 21–49 (2013)
40. Hjalmarsson, F., Pettersson, F.: Finite element analysis of cracking of concrete arch dams due to seasonal temperature variation. Master's thesis, Lund University (2017)
41. Honorio, T., Bary, B., Benboudjema, F.: Factors affecting the thermo-chemo-mechanical behaviour of massive concrete structures at early-age. Materials and Structures **49**(8), 3055–3073 (2016)
42. Hu, Y., Liang, G., Li, Q., Zuo, Z.: A monitoring-mining-modeling system and its application to the temperature status of the xiluodu arch dam. Advances in Structural Engineering **20**(2), 235–244 (2017)
43. Hu, Y., Zuo, Z., Li, Q., Duan, Y.: Boolean-based surface procedure for the external heat transfer analysis of dams during construction. Mathematical Problems in Engineering **2013** (2013)
44. Huang, Y., Xie, T., Li, C., Yin, X.: Optimization analysis of the position of thermometers buried in concrete pouring block embedded with cooling pipes. Mathematical Problems in Engineering **2019** (2019)
45. Husein Malkawi, A.I., Mutasher, S.A., Qiu, T.J.: Thermal-structural modeling and temperature control of roller compacted concrete gravity dam. Journal of performance of constructed facilities **17**(4), 177–187 (2003)
46. ICOLD: Bulletin 76. conventional methods in dam construction. Tech. rep., International Commission on Large Dams (1990). Google-Books-ID: 2zX0vgEACAAJ
47. ICOLD: Simulation of the thermo-mechanical effects occurring during the construction phases of a concrete arch dam. In: Proceedings of the Tenth ICOLD Benchmark Workshop on Numerical Analysis of Dams. Paris, France (2009)
48. ICOLD: Guidelines for use of numerical models in dam engineering, bulletin 155. Tech. rep., ICOLD (2013)
49. IDAE: Guía técnica - diseño de sistemas de intercambio geotérmico de circuito cerrado. Tech. rep., Instituto para la Diversificación y Ahorro de la Energía (2012)
50. Ishikawa, M.: Thermal stress analysis of a concrete dam. Computers & structures **40**(2), 347–352 (1991)
51. Jaafar, M., Bayagoob, K., Noorzaei, J., Thanoon, W.A.: Development of finite element computer code for thermal analysis of roller compacted concrete dams. Advances in Engineering Software **38**(11-12), 886–895 (2007)
52. Jin, F., Chen, Z., Wang, J., Yang, J.: Practical procedure for predicting non-uniform temperature on the exposed face of arch dams. Applied Thermal Engineering **30**(14), 2146–2156 (2010)
53. Kehlbeck, F.: Einfluss der Sonnenstrahlung bei Brückenbauwerken. Werner-Verlag (1975)
54. Khaneghahi, M.H., Alembagheri, M., Soltani, N.: Reliability and variance-based sensitivity analysis of arch dams during construction and reservoir impoundment. Frontiers of Structural and Civil Engineering **13**(3), 526–541 (2019)
55. Kuzmanovic, V., Savic, L., Stefanakos, J.: Long-term thermal two-and three-dimensional analysis of roller compacted concrete dams supported by monitoring verification. Canadian Journal of Civil Engineering **37**(4), 600–610 (2010)
56. Lamea, M., Mirzabozorg, H.: Evaluating sensitivity of an aar-affected concrete arch dam to the effects of structural joints and solar radiation. Strength of Materials **47**(2), 341–354 (2015)
57. Langtangen, H.P.: Computational partial differential equations: numerical methods and diffpack programming, vol. 2. Springer Science & Business Media (2013)
58. Lee, Y., Choi, M.S., Yi, S.T., Kim, J.K.: Experimental study on the convective heat transfer coefficient of early-age concrete. Cement and concrete composites **31**(1), 60–71 (2009)
59. Léger, P., Leclerc, M.: Hydrostatic, temperature, time-displacement model for concrete dams. Journal of engineering mechanics **133**(3), 267–277 (2007)
60. Leger, P., Venturelli, J., Bhattacharjee, S.: Seasonal temperature and stress distributions in concrete gravity dams. part 1: modelling. Canadian journal of civil engineering **20**(6), 999–1017 (1993)
61. Leitão, N., Tavares de Castro, A., Gomes da Cunha, J.: Analysis of the observed behaviour of Alto Ceira II dam during the first filling of the reservoir. In: Second International Dam World Conference. Lisbon, Portugal (2015)

62. Leitão, N.S.: Environmental thermal actions - thermal analysis of Alto-Lindoso dam. In: Proceedings of the 6th International Conference on Dam Engineering, p. 687–697. C. Pina, E. Portela, J. Gomes, Lisbon, Portugal (2011)
63. Leitão, N.S., Castilho, E.: Numerical modelling of the thermo-mechanical behavior of concrete arch dams during the first filling of the reservoir. In: M. Abdel Wahab (ed.) Proceedings of the 1st International Conference on Numerical Modelling in Engineering, pp. 238–253. Springer Singapore, Singapore (2019)
64. Li, L., Liu, X., Dao, V.T., Cheng, Y.: Thermal cracking analysis during pipe cooling of mass concrete using particle flow code. Advances in Materials Science and Engineering **2016** (2016)
65. Li, Q., Liang, G., Hu, Y., Zuo, Z.: Numerical analysis on temperature rise of a concrete arch dam after sealing based on measured data. Mathematical Problems in Engineering **2014** (2014)
66. Li, Q., Zuo, Z., Hu, Y., Liang, G.: Smart monitoring of a super high arch dam during the first reservoir-filling phase. Journal of Aerospace Engineering **30**(2), B4016001 (2016)
67. Lin, P., Li, Q., Hu, H.: A flexible network structure for temperature monitoring of a super high arch dam. International Journal of Distributed Sensor Networks **8**(11), 917849 (2012)
68. Liu, X., Li, T., Wang, Z., Zhao, L.: Study on influence factors of nonlinear finite element analysis for high arch dams. Applied Mathematics & Information Sciences **7**(2), 557 (2013)
69. Liu, X., Zhang, C., Chang, X., Zhou, W., Cheng, Y., Duan, Y.: Precise simulation analysis of the thermal field in mass concrete with a pipe water cooling system. Applied Thermal Engineering **78**, 449–459 (2015)
70. Liu, Y., Zhang, G., Zhu, B., Shang, F.: Actual working performance assessment of super-high arch dams. Journal of Performance of Constructed Facilities **30**(2), 04015011 (2015)
71. Luna, R., Wu, Y.: Simulation of temperature and stress fields during rcc dam construction. Journal of Construction Engineering and Management **126**(5), 381–388 (2000)
72. Malm, R.: Guideline for fe analyses of concrete dams. Tech. rep., Energyforsk (2016)
73. Malm, R., Hellgren, R., Ekstr om, T., Fu, C.: Cracking of a concrete arch dam due to seasonal temperature variations - theme a. In: Proceedings of the 14th ICOLD International Benchmark Workshop on Numerical Analysis of Dams, pp. 18–75. KTH Civil and Architectural Engineering, Stockholm, Sweden (2018)
74. Malm, R., Hellgren, R., Enzell, J.: Lessons learned regarding cracking of a concrete arch dam due to seasonal temperature variations. Infrastructures **5**(2), 19 (2020)
75. Mazumder, S.: Numerical methods for partial differential equations: finite difference and finite volume methods. Academic Press (2015)
76. Mehta, P.K.: Advancements in concrete technology. Concrete International **21**(6), 69–76 (1999)
77. Mirzabozorg, H., Hariri-Ardebili, M., Shirkhan, M., Seyed-Kolbadi, S.: Mathematical modeling and numerical analysis of thermal distribution in arch dams considering solar radiation effect. The Scientific World Journal **2014** (2014)
78. Mirzabozorg, H., Hariri-Ardebili, M.A., Shirkhan, M.: Impact of Solar Radiation on the Uncoupled Transient Thermo-Structural Response of an Arch Dam. Scientia Iranica **22**(4), 1435–1448 (2015)
79. Moghadas Jafari, R.: Dynamic analysis of arch dams : effect of thermal loading. Ph.D. thesis, University of British Columbia (2016)
80. Noorzaei, J., Bayagoob, K., Thanoon, W., Jaafar, M.: Thermal and stress analysis of kinta rcc dam. Engineering Structures **28**(13), 1795–1802 (2006)
81. Oñate, E., Nadukandi, P., Miquel, J.: Accurate FIC-FEM formulation for the multidimensional steady-state advection–diffusion–absorption equation. Computer Methods in Applied Mechanics and Engineering **327**, 352–368 (2017)
82. Pérez Castellanos, J.L., Martínez Marín, E.: La acción térmica del medio ambiente como solicitación de diseño en proyectos de presas españolas. Rev Obras Públicas **3349**, 79–90 (1995)
83. Ponce-Farfán, C., Santillán, D., Toledo, M.Á.: Thermal simulation of rolled concrete dams: Influence of the hydration model and the environmental actions on the thermal field. Water **12**(3), 19 (2020). DOI 10.3390/w12030858
84. de Pouplana, I., Oñate, E.: Finite element modelling of fracture propagation in saturated media using quasi-zero-thickness interface elements. Computers and Geotechnics **96**, 103–117 (2018)
85. Reinhardt, H., Hw, R., J, B.: Temperature development in concrete structures taking account of state dependent properties. In: Internatinal Conference on Concrete at Early Ages, pp. 211–218. Paris, France (1982)
86. Santillán, D.: Mejora de los modelos térmicos de las presas bóveda en explotación: aplicación al análisis del efecto del cambio climático. Ph.D. thesis, UPM (2014). In Spanish
87. Santillán, D., Salete, E., Toledo, M.: A methodology for the assessment of the effect of climate change on the thermal-strain–stress behaviour of structures. Engineering Structures **92**, 123–141 (2015)
88. Santillán, D., Salete, E., Toledo, M.: A new 1d analytical model for computing the thermal field of concrete dams due to the environmental actions. Applied Thermal Engineering **85**, 160–171 (2015)
89. Santillán, D., Salete, E., Vicente, D.J., Toledo, M.: Treatment of solar radiation by spatial and temporal discretization for modeling the thermal response of arch dams. Journal of Engineering Mechanics **140**(11), 05014001 (2014)
90. Sayed-Ahmed, E.Y., Abdelrahman, A.A., Embaby, R.A.: Concrete dams: thermal-stress and construction stage analysis. Dams and Reservoirs **28**(1), 12–30 (2018)
91. Schlicke, D., Kanavaris, F., Lameiras, R., Azenha, M.: On-site monitoring of mass concrete. In: Thermal Cracking of Massive Concrete Structures, pp. 307–355. Springer (2019)
92. Sheibany, F., Ghaemian, M.: Effects of environmental action on thermal stress analysis of Karaj concrete arch dam. Journal of Engineering Mechanics **132**(5), 532–544 (2006)
93. Shen, L., Ren, Q., Cusatis, G., Cao, M., Xu, L., Yang, Y.: Numerical study on crack thermal resistance effect on thermo-mechanical coupled behavior of concrete structure at room temperature. International Journal of Solids and Structures **182**, 141–155 (2020)
94. Silveira, A.: Temperatures variations in dams. Tech. rep., LNEC Memória nº 177 (1961)
95. Soltani, N., Alembagheri, M., Khaneghahi, M.H.: Risk-based probabilistic thermal-stress analysis of concrete

arch dams. Frontiers of Structural and Civil Engineering **13**(5), 1007–1019 (2019)
96. Stolz, D., Gortz, J., Wieprecht, S., Terheiden, K.: The influence of different thermal boundary conditions on the temperature distribution in concrete gravity dams. In: 26th ICOLD Congress (2018). Q101-R34
97. Su, H., Li, J., Hu, J., Wen, Z.: Analysis and Back-Analysis for Temperature Field of Concrete Arch Dam During Construction Period Based on Temperature Data Measured by DTS. IEEE Sensors Journal **13**(5), 1403–1412 (2013)
98. Tatin, M., Briffaut, M., Dufour, F., Simon, A., Fabre, J.P.: Thermal displacements of concrete dams: Accounting for water temperature in statistical models. Engineering Structures **91**, 26–39 (2015)
99. Tatin, M., Briffaut, M., Dufour, F., Simon, A., Fabre, J.P.: Statistical modelling of thermal displacements for concrete dams: Influence of water temperature profile and dam thickness profile. Engineering Structures **165**, 63 – 75 (2018)
100. Thelandersson, S.: Modeling of combined thermal and mechanical action in concrete. Journal of Engineering Mechanics **113**(6), 893–906 (1987)
101. Thomas, H., Zhou, Z.: Minimum time-step size for diffusion problem in fem analysis. International Journal for Numerical Methods in Engineering **40**(20), 3865–3880 (1997)
102. Torrenti, J., Buffo-Lacarrière, L.: On the variability of temperature fields in massive concrete structures at early age. In: 2nd International Symposium on Service Life Design for Infrastructures, pp. 893–900. RILEM Publications SARL (2010)
103. Townsend, C.L.: Control of Cracking in Mass Concrete Structures. United States Department of the Interior, Bureau of Reclamation (1965). Google-Books-ID: UJdctK5oXFMC
104. Ulm, F.J., Coussy, O.: Modeling of thermochemomechanical couplings of concrete at early ages. Journal of engineering mechanics **121**(7), 785–794 (1995)
105. USACE: Arch Dam Design. Engineer Manual 1110-2-2201. Tech. rep., Department of the Army. U.S. Army Corps of Engineers (1994)
106. USBR: Design criteria for arch and gravity dams. engineering monograph 19. Tech. rep., US Bureau of Reclamation (1977)
107. Vicente, D., San Mauro, J., Salazar, F., Baena, C.: An interactive tool for automatic predimensioning and numerical modeling of arch dams. Mathematical Problems in Engineering **2017** (2017)
108. Wang, Z., Liu, Y., Zhang, G., Yu, S.: Sensitivity analysis of temperature control parameters and study of the simultaneous cooling zone during dam construction in high-altitude regions. Mathematical Problems in Engineering **2015** (2015)
109. Wang, Z., Tao, L., Liu, Y., Yunhui, J.: Temperature control measures and temperature stress of mass concrete during construction period in high-altitude regions. Advances in Civil Engineering **2018** (2018)
110. Xu, Q., Chen, J.y., Li, J., Yue, H.y.: A study on the contraction joint element and damage constitutive model for concrete arch dams. Journal of Zhejiang University SCIENCE A **15**(3), 208–218 (2014)
111. Yang, J., Hu, Y., Zuo, Z., Jin, F., Li, Q.: Thermal analysis of mass concrete embedded with double-layer staggered heterogeneous cooling water pipes. Applied Thermal Engineering **35**, 145–156 (2012)
112. Zhu, B.: Prediction of Water Temperature in Deep Reservoirs. Dan Engineering **8**(1), 13–26 (1997)
113. Zhu, B.: Thermal stresses and temperature control of mass concrete. Elsevier, Oxford, UK (2014)
114. Zienkiewicz, O.C., Taylor, R.L., Zhu, J.Z.: The finite element method: its basis and fundamentals. Elsevier (2005)